

Power Distribution System for a CubeSat

*Project report
submitted to the APJ Abdul Kalam Technological University
in partial fulfillment of the requirements
for the degree of*

Bachelor of Technology in Electrical and Electronics Engineering



by

**Ansaf Niyaz
TRV19EE016**

**Govind Murali
TRV19EE025**

**Jijesh J. Kumar
TRV19EE029**

**Naveen A.B.
TRV19EE038**

**ELECTRICAL AND ELECTRONICS ENGINEERING
GOVERNMENT ENGINEERING COLLEGE, BARTON HILL**

JANUARY, 2023

DECLARATION

Project Title Power Distribution System for a CubeSat
Authors *Ansaf Niyaz, Govind Murali, Jijesh J. Kumar and Naveen A.B.*
Student IDs TRV19EE016, TRV19EE025, TRV19EE029, and TRV19EE038

We, the undersigned, hereby declare that the mini project report titled *Power Distribution System for a CubeSat*, submitted for partial fulfillment of the requirements for the award of degree of Bachelor of Technology of the APJ Abdul Kalam Technological University, Kerala is a bonafide work done by us under the supervision of Dr. Dinesh Gopinath, Department of Electrical and Electronics Engineering, Government Engineering College, Barton Hill. This submission represents our ideas in our own words and ideas and words of others have been included, we have adequately and accurately cited and referenced the original sources. We also declare that we have adhered to ethics of academic honesty and integrity and have not misrepresented or fabricated any data or idea or fact or sources in submission. We understand that any violation of the above will be a case for disciplinary action by the institute and/or the University can also evoke penal action from the sources which have thus not been properly cited or from whom proper permission has not been obtained. This report has not been previously formed the basis for the award of any degree, diploma or similar title of any other university

Place: TVM

Date: June 15, 2023

Ansaf Niyaz TRV19EE016
Govind Murali TRV19EE025
Jijesh J. Kumar TRV19EE029
Naveen A.B. TRV19EE038

Department of Electrical and Electronics
Engineering
Government Engineering College,
Barton Hill

**DEPT. OF ELECTRICAL & ELECTRONICS ENGINEERING
GEC BARTON HILL TRIVANDRUM**

2019-23



CERTIFICATE

This is to certify that the report titled **Power Distribution System for a CubeSat** submitted by **Ansaf Niyaz, Govind Murali, Jijesh J. Kumar, Naveen A.B.** of the **Department of Electrical and Electronics Engineering** to the APJ Abdul Kalam University in partial fulfillment of the requirements for the award of the Degree of *Bachelor of Technology in Electrical and Electronics Engineering* is a bonafide record of the project work carried out by them under my guidance and supervision. This report in any form has been submitted to any other university or institute for any purpose.

Dr. Dinesh Gopinath
(Project Guide)
Professor
Electrical and Electronics Engineering
GEC Barton Hill
Thiruvananthapuram

Prof. Beena N.
(Project Coordinator)
Assistant Professor
Electrical and Electronics Engineering
GEC Barton Hill
Thiruvananthapuram

Prof. Francis M. Fernandez
(Head of Department)
Professor
Electrical and Electronics Engineering
GEC
Barton Hill, Thiruvananthapuram

ACKNOWLEDGEMENTS

We would love to express our sincere gratitude to **Dr. Shiny G**, Principal, Government Engineering College, Barton Hill for giving us the opportunity to do the project work.

We owe a great deal of gratitude towards **Dr. Francis M. Fernandez**, Head of the Department of Electrical and Electronics Engineering, Government Engineering College, Barton Hill, for his whole hearted support for this project.

We express our sincere thanks and deep sense of gratitude to our project guide **Dr. Dinesh Gopinath**, Department of Electrical and Electronics Engineering, for his encouragement and support throughout our preparations.

We would like to extend our sincere gratitude to **Prof. Beena N**, Electrical and Electronics Engineering, Government Engineering College, Barton Hill, Trivandrum for her support and co-operation.

We also thank our colleagues who have helped us in partial completion of the project.

Ansaf Niyaz, Govind Murali , Jijesh J. Kumar and Naveen A.B.

Government Engineering College, Barton Hill

Date: June 15, 2023

ABSTRACT

CubeSats are miniature versions of satellites that offer hands-on experience to engineering students in designing, developing, testing and operating a real space-craft system. A 1U CubeSat is a cube shaped satellite with dimensions of 10 cm x 10 cm x 10 cm and maximum mass of 1.33 kilograms. CubeSats are traditionally built from COTS-components (Commercial Off-the-Shelf) with low resources. Typically, CubeSat have limited mission time and short development and testing time.

One of the most critical aspects of the CubeSat is the Electrical Power System (EPS) since the electrical power is necessary for a CubeSat to operate. The EPS of the CubeSat consists mainly of solar cells, batteries, voltage converters and protection circuits. The EPS is responsible of providing stable power to the CubeSat subsystems.

The purpose of this project is to design and implement an EPS for a CubeSat. The EPS must be able to power all subsystem components including telemetry, on-board computer, attitude determination and control system , thermal system as well as the payload while also protecting the subsystems from the over-current and over-voltage issues associated with the device failure. The system will be designed to provide power for the satellite throughout the entire orbit, even during periods of eclipse when the satellite is not able to generate power. The EPS should also provide data about voltage and current measurements, battery status, etc. to OBC (On-Board Computer).

ABBREVIATIONS

DC	Direct current
IC	Integrated Circuit
EPS	Electrical Power System
MCU	Micro-controller Unit
OBC	Onboard Computer
PCB	Printed Circuit Board
PWM	Pulse Width Modulation
RBF	Remove Before Flight
TCS	Thermal Control System
TTC	Telemetry, Tracking and Command
ADCS	Attitude Determination And Control System
MPPT	Maximum Power Point Tracking
OCPC	Over Current Protection Circuits
CCCV	Constant Current Constant Voltage
OVP	Over-Voltage Protection
RTOS	Real-time Operating System

Contents

List of Figures	ix
List of Tables	xi
1 Introduction	1
1.1 Background	1
1.2 Objective	3
1.2.1 The Satellite Research Center, GECB	3
1.3 Literature Review	4
2 The Electrical Power System	5
2.1 Requirements of EPS	5
2.1.1 Introduction	5
2.1.2 Constraints	6
2.1.2.1 Vacuum	6
2.1.2.2 Radiations	6
2.1.2.3 Temperature	8
2.1.2.4 Vibrations and Accelerations during launch	8
2.1.2.5 Temperatures during launch	8
2.2 Components of EPS	9
2.3 Tasks of EPS	10
3 Power Budget	11
4 System Architecture	14
4.1 Introduction	14
4.2 Selected Architecture	16

5 Component Selection and Design	18
5.1 Solar Panels	18
5.2 MPPT Circuit	19
5.2.1 PCB Layout	21
5.3 Battery	23
5.3.1 Battery Selection	23
5.4 Battery Charger	24
5.5 Switching Regulators	29
5.6 Protection Circuits	30
5.6.1 PCB Layout	32
5.7 Micro-controller	33
5.8 Component List	34
5.9 EPS PCB Design as per PC/104 Specifications	34
5.10 3D Model	41
6 Testing	43
6.1 Variable DC load using MOSFET	43
6.2 VirtualBench	44
6.3 Testing of DC/DC converters	44
6.3.1 Output line regulation	45
6.3.2 Output load regulation	51
6.3.3 Output over-current protection	57
6.3.4 Output over-voltage protection	58
6.3.5 Efficiency	58
6.4 Battery Charger Testing	59
6.5 MPPT Module Testing	61
7 Conclusion	65
7.1 Accomplished Work	65
7.1.1 Architecture	65
7.1.2 Design	65
7.1.3 Implementation and tests	66
7.2 Future Scope	66
References	67

List of Figures

4.1	CubeSat EPS architectures	15
4.2	System Architecture of the CubeSat EPS	16
5.1	MPPT circuit with SPV1040	21
5.2	MPPT PCB Design	22
5.3	MPPT 3D	22
5.4	K_{ICHG} vs. I_{CHG} characteristics	26
5.5	Schematic of Battery Charger circuit with BQ25302	27
5.6	Battery Charger circuit PCB - All Copper Layers only	27
5.7	Battery Charger circuit PCB - 3D Model	28
5.8	LTC3426 as boost IC and TPS62203 as buck IC	30
5.9	Schematic of Buck and Boost circuit with Protection and Voltage and Current Measurement ICs	31
5.10	Buck and Boost circuit PCB - All Copper Layers only	32
5.11	Buck and Boost circuit PCB - 3D Model	32
5.12	MPPT	35
5.13	Battery Charger	35
5.14	Power Regulation circuits	36
5.15	Protection eFuse circuits	37
5.16	Voltage and Current measurement circuits	38
5.17	STM32 Micro-controller	39
5.18	PC/104 Connection Pins (Only pins connected to the EPS are labelled)	40
5.19	3D Model of EPS PCB (Top Layer)	41
5.20	3D Model of EPS PCB (Bottom Layer)	42
6.1	Mosfet characteristics	43
6.2	Regulation module test setup	45

6.3	Buck output line regulation at full load (200 mA)	46
6.4	Buck output line regulation at no load	47
6.5	Buck output line regulation at half load(150 mA)	48
6.6	Boost output line regulation at full load (750 mA)	49
6.7	Boost output line regulation at half load (400 mA)	50
6.8	Testing of boost converter in 5 V rail	51
6.9	Boost load regulation at 3.6 V Vin	52
6.10	Boost load regulation at 4.2 V Vin	53
6.11	Boost load regulation at 5.0 V Vin	54
6.12	Buck load regulation at 3.6 V input	55
6.13	Buck load regulation at 4.8 V input	56
6.14	Buck load regulation at 6 V input	57
6.15	Battery charger test setup	60
6.16	Constant current and constant voltage charging	60
6.17	Variation of charging voltage and current while charging the 18650 Li-Ion battery upto 100%	61
6.18	MPPT test setup	62
6.19	MPPT output voltage at no load	62
6.20	MPPT output line regulation at half load (200 mA)	63
6.21	MPPT output line regulation at full load (400 mA)	64

List of Tables

3.1	Orbital Parameters	12
3.2	Power Budget	12
6.1	Buck output line regulation at full load (200 mA)	46
6.2	Buck output line regulation at no load	47
6.3	Buck output line regulation at half load(150 mA)	48
6.4	Boost output line regulation at full load(750mA)	49
6.5	Boost output line regulation at half load(400 mA)	50
6.6	Boost load regulation at 3.6 V Vin	52
6.7	Boost load regulation at 4.2 V Vin	53
6.8	Boost load regulation at 5.0 V Vin	54
6.9	Buck load regulation at 3.6 V input	55
6.10	Buck load regulation at 4.8 V input	56
6.11	Buck load regulation at 6 V input	57
6.12	MPPT output line regulation at half load (200 mA)	63
6.13	MPPT output line regulation at full load (400 mA)	64

Chapter 1

Introduction

1.1 Background

Artificial satellites are foundational components of modern society. Satellites have played a huge role in communication, navigation, scientific research, military surveillance and the study of the solar system and beyond.

Artificial satellites are launched into space using rockets and are placed in orbit around the Earth or other celestial bodies using thrusters. Once in orbit, they remain in space and continuously circle around the Earth, following a specific path called an orbit.

There are two main types of orbits for artificial satellites: geostationary orbit and low Earth orbit. Geostationary orbit is a circular orbit located at an altitude of approximately 36,000 kilometres above the Earth's equator. Satellites in this orbit appear to be stationary relative to a fixed point on Earth, making them ideal for communication and navigation purposes. Low Earth orbit, on the other hand, is an orbit located at an altitude of up to approximately 2,000 kilometres above the Earth's surface. Satellites in this orbit circle the Earth more frequently and are used for scientific research, remote sensing, and military surveillance.

Artificial satellites are powered by solar panels that convert sunlight into electricity, which is used to operate the satellite's systems and instruments. They are also equipped with communication antennas that enable them to transmit and receive signals from Earth or other satellites.

For more than a decade, CubeSats, or small satellites, have paved the way to low-Earth orbit for commercial companies, educational institutions, and non-profit organizations. These small satellites offer opportunities to conduct sci-

tific investigations and technology demonstrations in space in such a way that is cost-effective, timely and relatively easy to accomplish. Due to their small size, CubeSats can be launched on smaller rockets or piggybacked on larger missions, allowing for more frequent and flexible deployment opportunities. The small size of CubeSats allows for faster development and testing of new technologies, which can be later applied to larger satellites or space missions.

A CubeSat is a class of miniaturized satellite based around a form factor consisting of 10 cm cubes. CubeSats have a mass of no more than 2 kg per unit, and often use commercial off-the-shelf (COTS) components for their electronics and structure. CubeSats are put into orbit by deployers on the International Space Station, or launched as secondary payloads on a launch vehicle. As of August 2021, more than 1,600 CubeSats have been launched.

CubeSat missions benefit Earth in varying ways. From Earth imaging satellites that help meteorologists to predict storm strengths and direction, to satellites that focus on technology demonstrations to help define what materials and processes yield the most useful resources and function best in a microgravity environment, the variety of science enabled by CubeSats results in diverse benefits and opportunities for discovery.

Electrical power systems (EPS) are an essential component of CubeSats as they have a limited power budget and often require a reliable source of power to operate their payloads and subsystems. There are several ways to design an EPS for a CubeSat, and the choice depends on the mission requirements and the available resources. The most common EPS design for CubeSats is based on solar panels, which convert sunlight into electrical energy.

The solar panels are typically connected to a power management and distribution unit (PMDU), which regulates the voltage and current of the incoming power and distributes it to the various subsystems and payloads. The PMDU also includes a battery that stores excess power generated by the solar panels and provides power during eclipses or when the solar panels are not receiving enough sunlight.

The EPS also includes other components such as a power switch, a fuse, and a battery charge controller. The power switch is used to turn on or off the power to the subsystems and payloads, while the fuse protects against over-current and short circuits. The battery charge controller manages the charging and discharging of the battery, ensuring that it is not overcharged or over-discharged.

The design of the EPS depends on the specific mission requirements and the available resources, and CubeSat developers must carefully balance the power budget to ensure that the CubeSat can operate reliably and efficiently throughout its mission.

1.2 Objective

The aim of this project is to determine requirements for a typical CubeSat Electrical Power System (EPS) and develop a working prototype of the EPS for a CubeSat.

This EPS will be used as the prototype for the BARTOSAT cubeSat developed by the students of GEC, Barton Hill as a part of the Satellite Research Center of the college. The prototype will then go through various iterations, improving the design to meet all the requirements of other subsystems which are currently under development and also to make it fully capable to work in the space environment.

1.2.1 The Satellite Research Center, GECB

The Satellite Research Center of Government Engineering College, Barton Hill, is a facility dedicated to conducting research in the field of satellite technology and to help students get an exposure to space technologies in general. As a part of this, a student project was initiated, aimed at developing a 1U CubeSat named 'Bartosat', which will be designed to carry a LoRa module as the payload.

Every phase of designing, building and testing of the CubeSat has been carried out by different student teams from various departments. The payload will test the possibilities of space-to-ground communication using LoRa technology, which can lead to low cost, low-power space communication.

1.3 Literature Review

The EPS is a critical component of a CubeSat as it powers all the subsystems in the satellite. There are different EPS architectures based on DC bus regulation and interface of PV panels [1]. This project focuses on the design of an EPS with a regulated DC bus and MPPT tracking.

Based on the difference between centralized and distributed architectures discussed in [2], we have selected distributed architecture. Distributed architecture has various advantages like increased scalability, fault tolerance and often more cost effective than centralized architecture.

As discussed in [3], solar panels operate at their most efficient points with a power point tracking algorithm, allowing the extraction of maximum power from the solar panels. Hence, peak power transfer is preferred to direct power transfer. Various power point tracking algorithms were reviewed and Perturb and Observe algorithm was selected as the best option for the EPS design.

Different battery technologies used in CubeSats were discussed in [4] and Li-ion cells were selected as the energy storage device due to their high energy density and higher number of charge discharge cycles compared to LiPo and NiMH batteries.

From [5], the optimum ambient temperature for charging a Lithium ion battery is +5°C to +45°C and thus, charging is limited to this range of temperature. Various charging methods were also reviewed for selecting the IC's which can implement the best battery charging method.

Chapter 2

The Electrical Power System

The Electrical Power System (EPS) is an electronic circuit board that is designed to supply, manage and store energy in an efficient way. The EPS must be able to harvest energy from the solar panels and store it in the battery, as well as delivering power to the satellite, using switch controlled converters to supply a regulated voltage. Redundant circuitry must be present to ensure continuous and reliable operation of the satellite in case of the failure of EPS components.

The output of the solar panels is first run through the power path control. While in sunlight operation, the power path will select the voltage from the panels based on its higher voltage. The output of the Power Path control is sent to DC-DC converters to provide 5V and 3.3V regulated DC supply for the CubeSat modules. During the eclipse, the power path will select the battery to power the circuit components. The software is implemented in order to manage the overall energy of the satellite, regulate the converters to extract maximum power from solar panels, perform power diagnostics, engage redundant circuitry and to communicate with the On Board Computer. The software also employs four operating modes: Initialization mode, Safe mode, Normal mode and Low Power Mode.

2.1 Requirements of EPS

2.1.1 Introduction

The first step before beginning the design of the EPS is to know exactly what our goals and our constraints are. This is the subject of this section.

There are constraints due to space environment. The EPS must withstand vacuum and wide ranges of temperatures and radiations. There are constraints linked to the launch, like accelerations, vibrations, and rules for the CubeSats in the launch vehicle. Finally, there are constraints due to the construction of CubeSat itself. The dimensions of the PCB and available volumes should be specified.

The desired functionalities also guide the design. The EPS must produce enough energy to supply the CubeSat. Enough energy has to be stored to supply the satellite during the period of eclipse. The EPS must provide several power outputs with stabilized voltages. The constraints will also guide the validation tests applied to the prototypes. Since our objective is to make demo boards, all these constraints may not be fully follower while designing.

2.1.2 Constraints

2.1.2.1 Vacuum

The satellite is expected to be released in an elliptical orbit with an altitude between 350 and 1,000 km. At such altitudes, the atmosphere pressure can be neglected and considered as vacuum. Therefore, all components used in the satellite must withstand vacuum. The most sensitive component of the EPS is the batteries. The two threats of vacuum are:

- Deformations due to mechanical constraint of vacuum
- Out gassing.

2.1.2.2 Radiations

Charged particles of solar wind, electrons, and protons, are captured by the earth magnetic field. They form the radiations belts, also known as the Van-Allen belts. There are two belts:

- The inner belt, between 1,000 and 15,000 km, containing high concentrations of energetic protons with energies exceeding 100 MeV and electrons in the range of hundreds of keV.

- The outer belt, extending till 50,000 km, and consisting mainly of high energy electrons (from 0.1 to 10 MeV).

Spacecrafts need to be protected against radiations, especially if they go through the radiation belts. Trapped particles in the radiation belts and cosmic rays can cause “Single Event Phenomena” (SEP) within semiconductor devices. There are three different types of SEP:

- The Single-Event Upset (SEU)
 - This is when a high energy particle hits a logic device and changes digitally stored data or causes a gate to open or close at the wrong time.
- The Single-Event Latch up (SEL)
 - The SEL is when a high energy particle directly damages the device. It can, however, be corrected if the SEL is detected and the power to the device quickly turned off, then turned back on.
- The Single-Event Burnout (SEB)
 - This is the case where the device is destroyed.

The radiation dose is estimated to be more than 105 Sv. A protection against SEL can be provided to the subsystems with current-limiter circuits. There is no particular protection against SEU and SEB except reducing the effect of the radiations inside the satellite with a layer of shielding aluminium (less than 2.104 Sv with 2mm of aluminium). There are components designed and/or tested to be more resistant to radiations. Such components should be used in the more critical systems of the EPS.

2.1.2.3 Temperature

The temperatures in space, when the satellite is turned on, will essentially depend of the thermal design. The temperature ranges are not the same everywhere in the satellite. Thermal simulations give an idea of the temperature at different points of the CubeSat. The external temperature will vary the most (from -33°C to $+40^{\circ}\text{C}$), the temperature of the EPS will stay between -22°C and $+37^{\circ}\text{C}$, and the temperature of batteries between -22°C and $+37^{\circ}\text{C}$. The EPS must thus be able to work within these ranges.

- Solar cells must be selected so that they are able to work in the predicted range of -33°C to $+40^{\circ}\text{C}$.
- The electronics on the EPS must be designed to be able to operate from -22°C to $+37^{\circ}\text{C}$ (PCB Temp). Considering wider ranges, components with an operating temperature range of at least 40°C to $+85^{\circ}\text{C}$ can be selected as "absolute maximum rating".
- Lithium-Polymer batteries can withstand 0 to $+45^{\circ}\text{C}$ during charge and -20°C to $+60^{\circ}\text{C}$ during discharge (but with a significant loss of capacity under 0°C). A solution must be found to maintain the batteries in these ranges of temperature.

2.1.2.4 Vibrations and Accelerations during launch

The CubeSat will be subjected to vibrations during the launch. The effects of acceleration during launch are not to be underestimated. The CubeSat has to be able to withstand an acceleration of 15 g, even if it will probably be lower in reality. Special attention must be paid to the fixation of heavy components. Also, components could be damaged by the bending of the PCB under vibrations and accelerations. Automotive components will be chosen whenever possible.

2.1.2.5 Temperatures during launch

The launch vehicle will pass through several atmospheric layers with specific temperatures. Inside the launch vehicle, the CubeSat will endure temperatures of -40°C to 80°C during launch. Components of the EPS have to be able to withstand

such temperatures during storage (the CubeSat is inactive during launch). Components with a working temperature range of -40°C to 85°C should not have any problems. The batteries are still the most sensible component. Their storage temperature should stay between -20°C and 60°C . A passive solution must be found to protect them during launch. Thermal insulation and thermal inertia will certainly help.

2.2 Components of EPS

The EPS of a CubeSat can be designed with many different architectures, but some components are common to all designs, such as:

- Solar panels to harvest the energy from the Sun
- Battery charger to manage the charging profile of the battery
- Voltage regulators to feed the regulated power bus of the satellite
- Remove Before Flight (RBF) switches and deployment switches, to cut the power while the satellite is not deployed

Other components of the EPS are:

- Battery and associated charging circuit
- Solar panels on 6 faces of the satellite
- MPPT converters which help optimise power collection from the sun
- Buck and boost converters which help provide required voltage busses for components of different voltages
- An MCU which controls the tasks that the EPS performs and monitors the status of the components
- Over Current Protection Circuit which helps protects important components from high current flow
- Current and Voltage sensors to keep track of their consumption.

- Temperature sensors to measure battery temperature, based on which battery heater is used
- Battery heater circuit

2.3 Tasks of EPS

Tasks of the EPS are:

- Collect housekeeping for various components associated with it, like the various current & voltage sensors and the battery's state of charge.
- Handle housekeeping requests and other commands from the OBC (ON/OFF requests of any subsystem by OBC).
- Implement MPPT to optimize power generation.
- Control the Simple Beacon (which contains only the call sign of the satellite) before the TTC gets switched on.
- Implement a watchdog timer to keep a check on the operation of the OBC.
- Take action on the basis of OCPC triggers.
- Deployment of antenna at the time of satellite initialisation.
- Turn on the battery heater when temperature goes below critical level

Chapter 3

Power Budget

The power budget of a CubeSat is a critical aspect of its design and operation, as it determines the capabilities and limitations of the satellite. A well-designed power budget can ensure that the CubeSat operates efficiently and achieves its mission objectives, while a poorly designed power budget can lead to power shortages and mission failure.

It is important to determine the power budget at the beginning of the EPS design to determine the characteristics of the system. When the available space for the solar cells and the orbital parameters are known, power production can be estimated. The power requirements of CubeSat as a whole depend upon the power requirements of the individual components and how the components are used together for operations. Together with the efficiency information of the EPS components, this data is used to determine critical elements of the EPS design, like required solar array and battery size.

A CubeSat will have standard set of satellite subsystems: Structural subsystem, Telemetry, Electrical Power Subsystem (EPS), Thermal Control Subsystem (TCS), Attitude Determination and Control Subsystem (ADCS), On Board Computer (OBC) and Payload. For the calculations, a LoRa module was selected as the payload. The orbital parameters are given below:

Parameter	Value
Orbital altitude	590 km
Orbital radius	6968.14 km
Flight velocity	7.563 km/s
Orbital period	96.483 min
Eclipse time	31.164 min
Daylight time	65.319 min

Table 3.1: Orbital Parameters

The CubeSat has an orbital altitude of 590 km with an orbital radius of 6968.14 km to maintain a flight velocity of 7.563 km/s. The orbital period is 96 min 29 sec with an eclipse time of 31 min 10 sec and daylight time of 65 min 19 sec. Based on the power budget, the energy required by the CubeSat is 1.997 Wh per orbit. Hence, the solar panels must be designed to produce at least 1.997 Wh per orbit.

Power requirements of various components of each subsystems are given below. Since the power production may vary due to parameters like efficiency of panels, margin and contingency are added to the total power requirements.

Sub-system		Voltage (V)	Max. Current (mA)	Power (mW)	Contingency 5%	Margin 20%	Duty Cycle (%)	Energy (Wh)
ADCS	ADCS	3.3	20	66	69.3	83.16	100	0.133725438
	Magnetorquer	3.3	100	330	346.5	415.8	50	0.334313595
OBC	OBC	5	40	200	210	252	100	0.4052286
Rx-Tx	Telemetry	5	300	1500	1575	1890	11	0.334313595
	Beacon	5	20	100	105	126	100	0.2026143
	GPS	3.3	40	132	138.6	166.32	30	0.0802352628
Payload	LoRa	5	20	100	105	126	10	0.02026143
EPS	EPS	-	-	160	168	201.6	100	0.32418288
	Thermal	-	-	250	262.5	315	32	0.16209144
					Tot Power(mW)	3575.88	Tot. Energy	1.997

Table 3.2: Power Budget

Conventionally, EPS will work on different modes to manage the overall power production and distribution of the CubeSat. The main modes are initializing mode, which is during the initial phase of CubeSat launch and the normal mode, which

is the rest of the mission. The initializing mode is divided into three: **Pre- Launch mode, Launch mode and Initializing mode.**

In pre launch mode, all subsystems are off. In launch mode, that is when the CubeSat is deployed into orbit, the EPS and OBC turns on. Then, during initializing, all subsystems are turned on for a small amount of time to check whether all subsystems are working properly.

The normal mode consists of safe mode and nominal mode.

During safe mode, only the EPS and beacon of telemetry system works, and the CubeSat is in a power saving mode. The nominal mode is the general purpose mode where payload will function.

To calculate battery and solar panel specifications, the peak power budget of the CubeSat is only considered since the power requirements won't exceed that requirements. The other modes are only documented for designing the functioning of micro-controller which controls the EPS. Of all the modes, highest power consumption during sun phase is when transmission and payload active (1.016 Wh), and highest power consumption during eclipse phase is when transmission and payload active (0.769 Wh).

From the peak power budget table, the highest energy requirement is 2.307 Wh.

Chapter 4

System Architecture

4.1 Introduction

The main challenge for the development of CubeSats is to fit all the necessary equipment within the standard frame size while meeting the weight constraints. The EPS design is crucial for the successful CubeSats mission, which needs to consider several factors such as mission duration, orbit altitude, inclination angle, size of PV panels and its arrangement, load profile, volume and weight limits, radiation effects, overall efficiency, simplicity of control, component count, flexibility in battery configuration, reliability, and fault-tolerant capability.

One of the important steps in EPS design is the selection of most suitable EPS architecture. The different types of CubeSat EPS architectures are shown in Figure.

Based on the interfacing of PV panels, the EPS architectures are classified as direct energy transfer (DET) and peak power tracking (PPT) architectures.

In the DET architecture, the PV panels are directly connected to the battery and/or load equipment via diodes. It also uses a shunt regulator in parallel with the PV panels to absorb excess power when the battery reaches full-charge condition.

In the PPT architecture, the PV panels are interfaced with a power electronic converter to extract the maximum power from the panels under widely varying op-

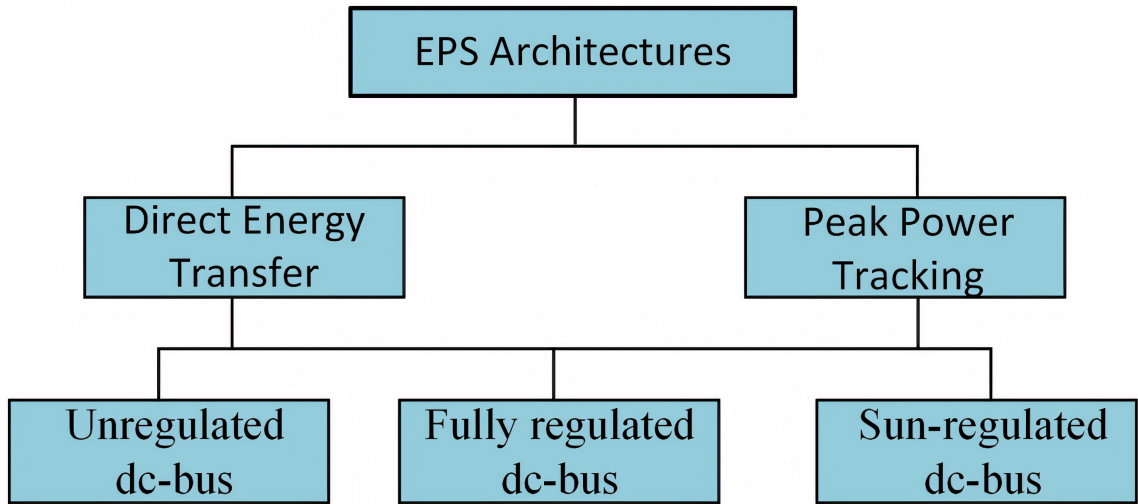


Figure 4.1: CubeSat EPS architectures

erating conditions such as solar irradiation, PV panel temperature, and inclination angle.

The DET architecture requires matching of PV panel characteristics and the dc-bus voltage to generate maximum possible power which is not straightforward in the space missions. Therefore, the majority of CubeSats utilize the PPT architecture to maximize the solar energy harvest, which has limited PV panel capacity and storage capacity due to strict volume and weight constraints.

The PPT architectures are further classified based on dc-bus voltage regulation: unregulated dc-bus, regulated dc-bus; and sun-regulated dc-bus.

The unregulated dc-bus EPS architecture has the battery terminals directly connected to dc-bus. When the battery voltage reaches its upper limit, the MPPT converter is operated in voltage regulation mode to avoid further charging of the battery.

The regulated dc-bus EPS architecture interfaces the battery with a dc-dc converter to maintain the dc-bus voltage at the predefined value. This architecture enables the operation of CubeSat at higher dc-bus voltage so that conduction and ohmic

losses are reduced.

In the sun regulated dc-bus EPS architecture, the dc-bus voltage is maintained at reference value only during the sunlit period. During the eclipse period, the battery gets connected to the dc-bus via a diode to supply the loads.

4.2 Selected Architecture

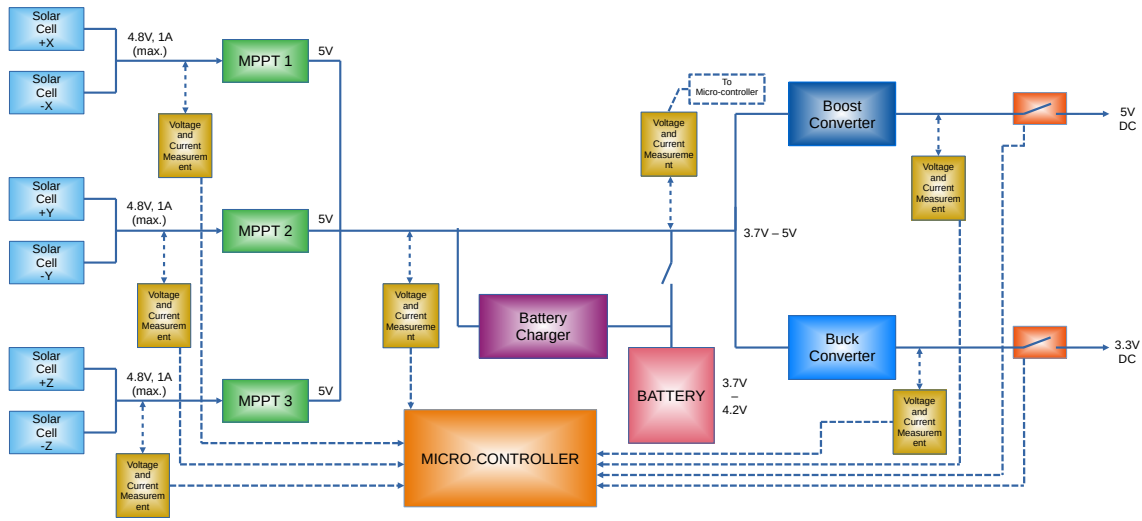


Figure 4.2: System Architecture of the CubeSat EPS

The electrical power system (EPS) is a critical component of CubeSat architecture, as it provides power to all the satellite's systems and payloads. EPS architecture of a CubeSat is designed to be highly efficient and reliable, while minimizing the mass and power consumption of the components. The EPS must be carefully designed and tested to ensure that it can withstand the harsh space environment and meet the mission requirements.

The CubeSat is equipped with six solar panels on each side. To ensure that the solar panels operate at their most efficient points, the solar panels are connected to MPPT ICs such that the solar panels on the opposite sides are connected to single MPPT IC. Since only one of the opposite sides of the cube is irradiated at any time,

the MPPT of two solar panels can be achieved using a single IC. This arrangement reduces the number of MPPT ICs required by the system. The MPPT runs a constant voltage algorithm and delivers 5 V at the bus.

When the CubeSat is capable of generating enough power through the solar panels, the components are directly powered by the panels through the bus. At the same time, a battery charging IC uses some of the energy to recharge the Li-ion cell. The battery charger takes the 5V from the bus and converts it to the voltage and current optimal for battery charging depending on the state of charge, temperature of the cell etc. During eclipse the battery power the energy from the panels is absent and the battery powers the CubeSat components. The voltage of the battery varies from 3.7 V to 4.2 V.

The buck and boost converters provide power to the 3.3 V and 5 V rails respectively. Their input voltage varies from 3.6 V to 5 V to account for direct power from the panels when sunlight is available and for battery power during eclipse.

To ensure proper functioning and to identify any faults in the system, there are various voltage and current measurement units placed at various points in the circuit. They measure the current and voltage at each point and the data is fed to a micro-controller, which is programmed to open the switches at the rails in case of any faults.

Chapter 5

Component Selection and Design

5.1 Solar Panels

TJ Solar Cell 3G30C - Advanced is selected. This cell is a GaInP/GaAs/Ge on Ge substrate triple junction solar cell. The end-of-life version of the 3G30C solar cell offers best EOL-performance values. Connected to the EPS via an external bypass diode protection.

Specifications:

- Average Open Circuit Voltage: 2.7 V
- Maximum Power Point Voltage: 2.41 V
- Average Short Circuit Current: 520.2 mA
- Maximum Power Point Current: 504.4 mA

It has an average efficiency of 29.8% at 1353 W/m^2 . This solar cell is excellent for space applications.

Since a CubeSat has six sides and one cell of selected model fits half of a side, a total of 12 cells can be placed.

Power from a solar panel, P :

$$P = P_i \times \text{Area} \times \eta \times \cos\alpha$$

Where,

P_i = incident power from sun (1367 W/m^2 at Low Earth Orbit)

η = conversion efficiency of cell (take 20% for contingency)

α = angle between normal of cell and incident light (avg: 35°)

Area of solar cell at one face : $0.0032 * 2 = 0.0064 \text{ m}^2$

Therefore, $P = 1367 \text{ W/m}^2 \times 0.0064 \times 20 \times \cos 35^\circ = 1.43 \text{ W}$

Assume two faces of CubeSat is lit by sunlight every time except eclipse and total sun time(T_s) is 1 hour (from orbital parameters).

Therefore, total energy produced is, $P \times T_s = (1.43 \times 2) \times 1 = 2.86 \text{ Wh}$

Of all modes specified in power budget, nominal mode at sun phase with transmission and payload ON consumes the most energy (1.016 Wh), and most energy consumed at eclipse phase is 0.769 Wh. This add upto 1.785 Wh, which is the worst case energy demand. This can be compensated by the designed solar panel configuration.

Solar panels are connected in such a way that each side has two cells connected in series. The maximum voltage developed per side is 4.4 V and the maximum current that can be generated per side at peak power point is 0.5 A. Panels on opposite sides are connected in parallel.

5.2 Maximum Power Point Tracking Circuit

Maximum Power Point Tracking (MPPT) is a technique used in photovoltaic (PV) systems to optimize the power output of the PV panel. The goal of MPPT is to ensure that the PV panel operates at its maximum power point (MPP), which is the point on the current-voltage (I-V) curve of the panel where the panel can produce the maximum amount of power.

As each solar panel has different temperatures and incident radiance angles, the Maximum Power Point (MPP) is also different. So each solar panel has a MPPT

converter to assure that the maximum power available at the solar panels is transferred independently from their working power points. Since the peak power point cannot be accurately predicted, many different algorithms exist for finding the best approximation. MPPT controllers use different algorithms such as **Perturb and Observe (P&O)**, **Incremental Conductance**, and **Fuzzy Logic** to track the MPP. These algorithms operate by incrementally changing the load impedance of the panel and measuring the corresponding change in voltage and current until the MPP is reached.

The SPV1040 was chosen as the MPPT IC. It is a boost converter with duty ratio controlled by Perturb and Observe MPPT algorithm. The perturb and observe algorithm is based on monitoring either the voltage or the current supplied by the DC power source unit so that the PWM signal duty cycle is increased or decreased step-by-step according to the input power trend. This chip has inbuilt over-current protection and a cutoff mechanism if the solar panel connection is reverse-inserted to prevent damage to the IC and the external circuit.

The MPPT IC can only handle 1.8 A of input current. Also, the input voltage of each MPPT must be much less than the desired output voltage for them to function properly. Depending on the configuration, the number of MPPT ICs was calculated to be 6.

Each side of cubesat consists of two 2.4 V cells, each cells giving a maximum current output of 500 mA for each MPPT, which is well below the maximum current the IC can handle. One cell from opposite sides are connected to its own MPPT, which is set to boost to 5.2 V. The MPPTs are then connected in parallel.

Connecting multiple regulators in parallel can sometimes cause problems if one source is outputting a slightly smaller or larger voltage than the others. In most cases, the use of ballast resistors solves this problem. The footprint for a 25 mohm ballast resistor will be chosen to be included in series with the output of each MPPT.

Specifications of SPV1040 [7]:

- Input Voltage: 0.3 - 5.5 V
- Output Voltage: 5 V
- Switching Frequency: 100 kHz
- Efficiency: 95%

The MPPT circuit schematic is shown below:

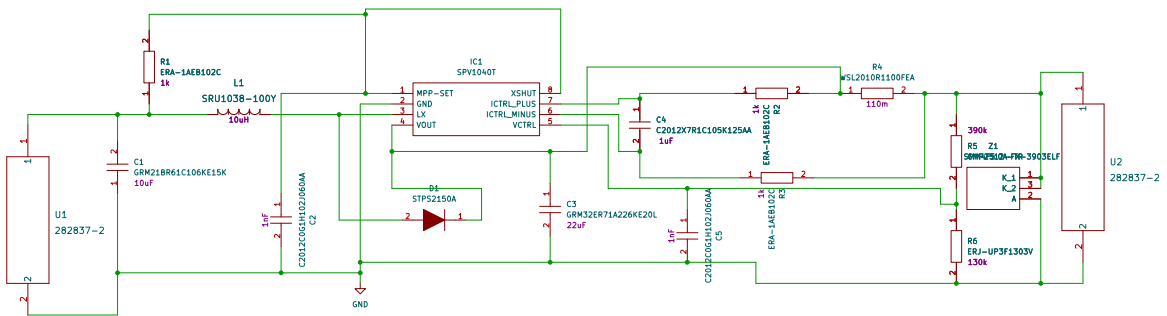


Figure 5.1: MPPT circuit with SPV1040

5.2.1 PCB Layout

The PCB was designed in KiCad EDA software. The MPPT PCB layout is shown below:

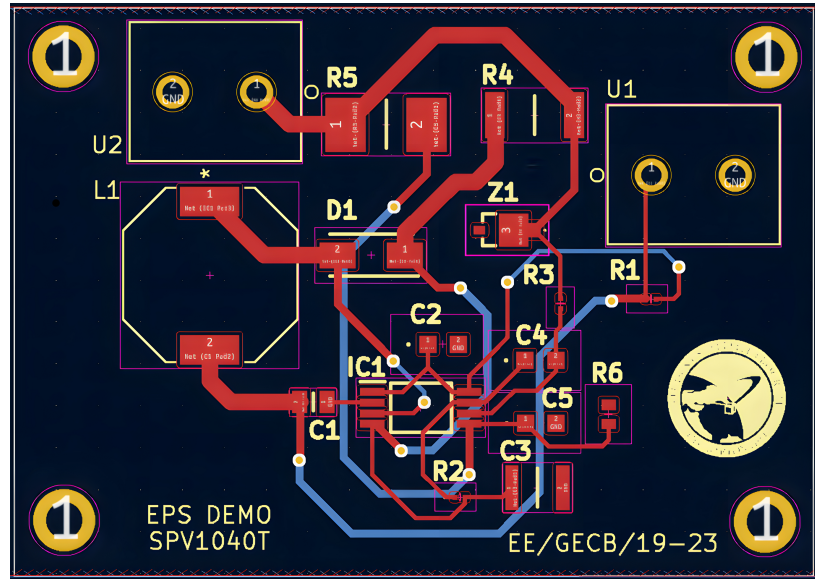


Figure 5.2: MPPT PCB Design

The 3D model of the MPPT PCB is shown below:

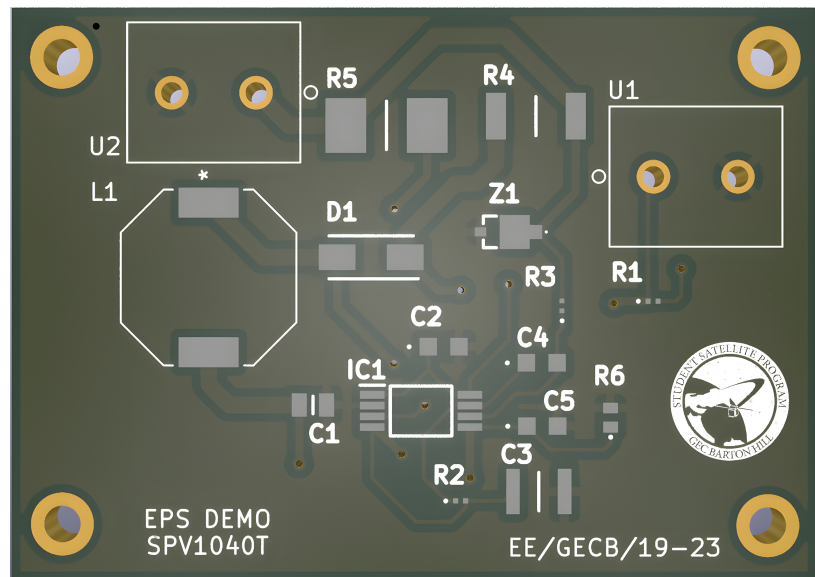


Figure 5.3: MPPT 3D

5.3 Battery

The most popular types of batteries use the following materials: Nickel Cadmium (NiCd), Nickel Metal Hydride (NiMH), Nickel Hydrogen (NiH₂), Lithium Ion (Li-Ion) and Lithium Polymer (Li-Po). The Li-Po and Li-Ion became the standard use in space technology due to their high energy density (Upto 200 Wh / kg on Li-Po and upto 250 Wh / kg on Li-Ion) and also due to the number of charging cycles being as high as the NiMH, whilst presenting higher operating temperatures.

5.3.1 Battery Selection

According to solar power calculations, the solar panel can produce 2.86 Wh of energy in a single orbit, of which 1.016 Wh will be used up in sun phase in worst case (E_{max}). So there will be atleast 1.844 Wh of energy left to charge the battery.

In power budget, the most amount of energy required during eclipse phase is 0.769 Wh.

Assign 50% contingency, the battery needs energy of 1.1535 Wh for charging, to use in worst case eclipse mode. This energy corresponds to 30% of total battery capacity (End Of Life capacity of battery).

So, we need a battery with Beginning Of Life capacity of 3.845 Wh.

$$\text{Required Ah of battery} = \frac{\text{Estimated Wh}}{\text{Battery Voltage}}$$

$$\text{So, required Ah} = \frac{3.845\text{Wh}}{3.6V} = 1.068 \text{ Ah}$$

Considered options are Samsung 18650 and Panasonic 18650 Li-ion cells. Samsung 18650 has 2500 mAh capacity, 3.6 V and a capacity loss of 60% after 250 charging cycles ($N_{in}=250$). Panasonic 18650 has 3350 mAh capacity, 3.6 V and a capacity loss of 60% after 300 charging cycles ($N_{in}=300$).

for a CubeSat mission of 3 months, required battery cycles will be around 1460 cycles (since each day, CubeSat goes through 16 sun phase).

Total no. of cycles a cell can provide = N_T

$$N_T = \frac{N_{in} \times C_B}{C_{exp}}$$

Where,

N_{in} = initial number of cycles a battery can provide)

C_B = Capacity of the battery

C_{exp} = Capacity expected to use

$$C_{exp} = \frac{E_{max}}{V_B}$$

Where,

E_{max} = Maximum energy consumed in a phase with 50% contingency

V_B = Battery voltage

Therefore, $C_{exp} = \frac{1.524}{3.6V} = 450$ mAh

Total no. of cycles Samsung 18650 can provide = $\frac{250 \times 2500}{450} = 1388$ cycles

Total no. of cycles Panasonic 18650 can provide = $\frac{300 \times 3350}{450} = 2200$ cycles

Therefore, Panasonic 18650 is selected, as it can compensate the charging cycle requirements. Specifications of Panasonic NCR 18650 GA Li-Ion cell:

- Voltage: 3.7 V - 4.2 V
- Capacity: 3500 mAh
- Can withstand 2200 charge-discharge cycles
- 1800 cycles till capacity reduces to 60%

5.4 Battery Charger

The battery also needs a charger to regulate its current and voltage while charging. BQ25302, a synchronous Buck Battery Charger IC was selected and connected in external power path mode as given in the data-sheet. The BQ25302 is a highly-integrated standalone switch-mode battery charger for single cell Li-Ion batteries. It supports input voltage in the range of 4.1 V to 6.2 V and maximum charging

current of 2 A. It has a very low quiescent current of 200 nA to conserve battery during idle. It detects the charge voltage setting at startup and charges the battery in four phases: battery short, pre - conditioning, constant current, and constant voltage.

The charger incorporates various safety features for battery charging and system operations, including battery temperature monitoring based on negative temperature coefficient (NTC) thermistor, charge safety timer, input over-voltage and over-current protections, as well as battery over-voltage protection. Thermal regulation regulates charge current to limit die temperature during high power operation or high ambient temperature conditions.

The STAT pin output reports charging status and fault conditions. It is connected to REGN via a current limiting resistor and LED. Blinking LED indicated a fault condition.

The battery charge voltage setting is done by the VSET pin. As the Panasonic NCR 18650 GA Li-Ion cell with a charge voltage of 4.2 V was selected the VSET pin was shorted to ground to set the battery charge voltage to 4.2 V.

To preserve battery life, the charging current has to be limited. The charging current provided to the battery by BQ25302 IC can be limited by adjusting the resistor value at the ICHG pin according to the equation below:

$$I_{CHG}(A) = K_{ICHG}(A.\Omega)/R_{ICHG}(\Omega) \quad (5.1)$$

Where,

- I_{CHG} is the charging current
- K_{ICHG} is the charge current ratio. The K_{ICHG} vs. I_{CHG} typical characteristic curve is shown in fig. 5.4
- R_{ICHG} is the resistor value at the ICHG pin

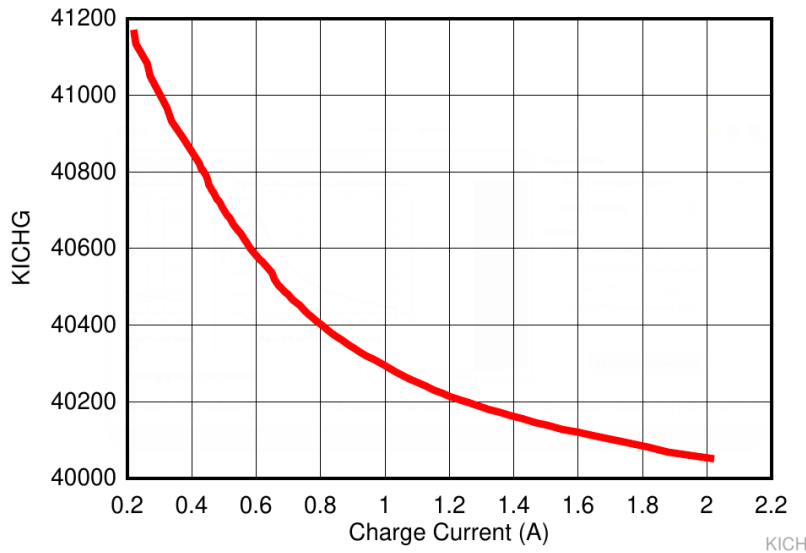


Figure 5.4: K_{ICHG} vs. I_{CHG} characteristics (Source: [8])

From the fig. 5.4, it is clear that the value of K_{ICHG} should be 40200 to limit the charging current near to 1.2 A. Thus, from equation 5.1 the calculated value of resistance at the ICHG pin is 33.5 k Ω .

The IC is connected in an external power path configuration by connecting an external PFET for the battery. The PFET turns on when there is no external supply available from the solar panels and the system has to be powered by the battery. It is also useful if the system has to be powered ON when the battery is over-discharged or dead.

Specifications and Operating Conditions of BQ25302 [8]:

- Input Voltage: Upto 5 V
- Output Voltage: Upto 4.2 V
- Switching Frequency: 1.2 MHz
- Output Current: Limited to 1.2 A by connecting a 33.5k resistor at ICHG pin
- Efficiency: 94.3% at 1A from 5 V input
- Thermistor: Semitec 103AT-2 (10k Ω)

- Charging Temperature: Limited between 0 - 45 °C

The Battery Charger circuit schematic is shown below:

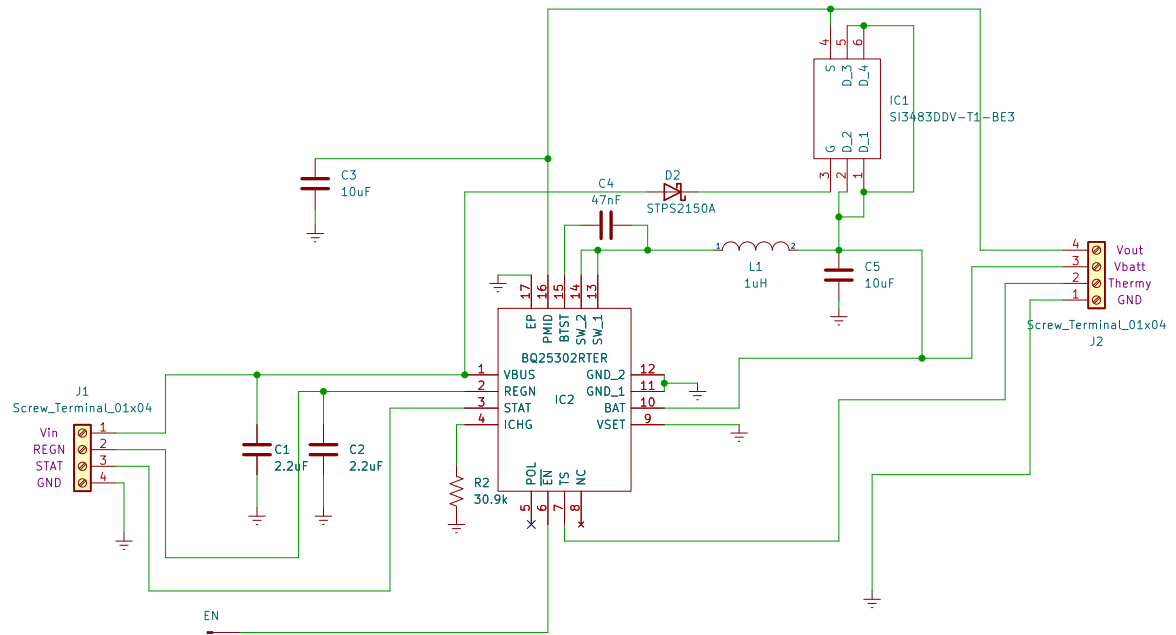


Figure 5.5: Schematic of Battery Charger circuit with BQ25302

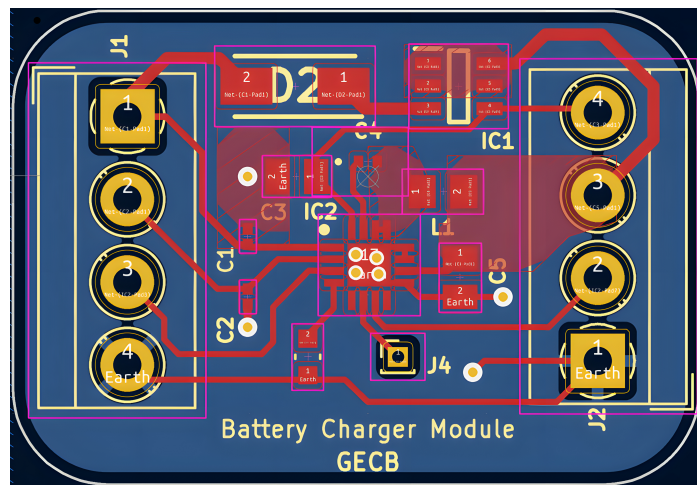


Figure 5.6: Battery Charger circuit PCB - All Copper Layers only

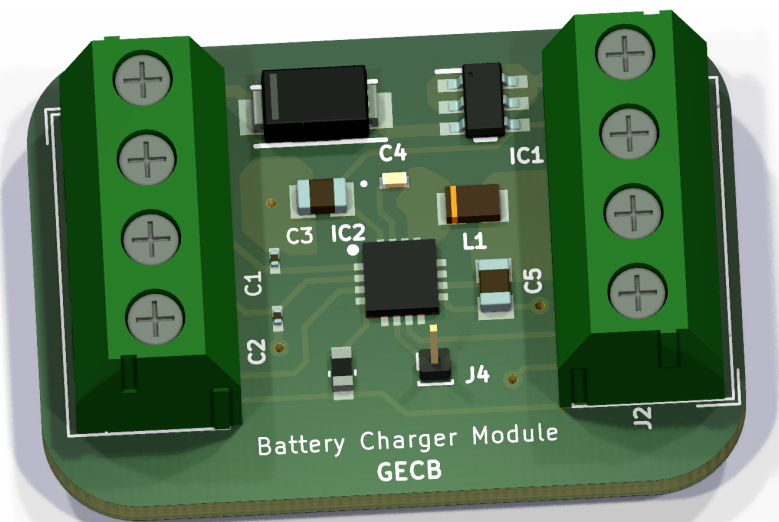


Figure 5.7: Battery Charger circuit PCB - 3D Model

5.5 Buck and Boost Converters

The power conditioning is associated with regulating the voltage to accommodate for the charging voltage and the voltages of the satellite's subsystems. In most subsystems, the need for a specific voltage requires a regulation of either a step-up or a step-down of the supplied voltage. It can be done by buck convertor(step-down) and boost converter(step-up).

TPS62203 was selected as the buck converter to provide step down voltage of the DC bus to supply the 3.3 V loads. It is a high-efficiency synchronous step-down converter with up to 95% efficiency. It operates with a 1MHz fixed frequency (PWM) at moderate loads to heavy load currents and operates with pulse frequency modulation (PFM) at light load currents.

It has a shutdown quiescent current of typically $0.1 \mu\text{A}$

Specifications and Operating Conditions of TPS62203[9]:

- Input Voltage: 3.6 - 5 V
- Output Voltage: 3.3 V
- Switching Frequency: 1 MHz
- Output Current: 300 mA (max.)

LTC3426 was selected as the boost converter to provide step up voltage of the DC bus to supply the 5V loads. It has an internal 2 A MOSFET as the switch.

Specifications and Operating Conditions of LTC3426[10]:

- Input Voltage: 3.6 - 5 V
- Output Voltage: 5 V
- Switching Frequency: 1.2 MHz
- Output Current: 500 mA (max.)

All convertors operate in continuous conduction mode.

The Buck and Boost Converter circuit schematic is shown below:

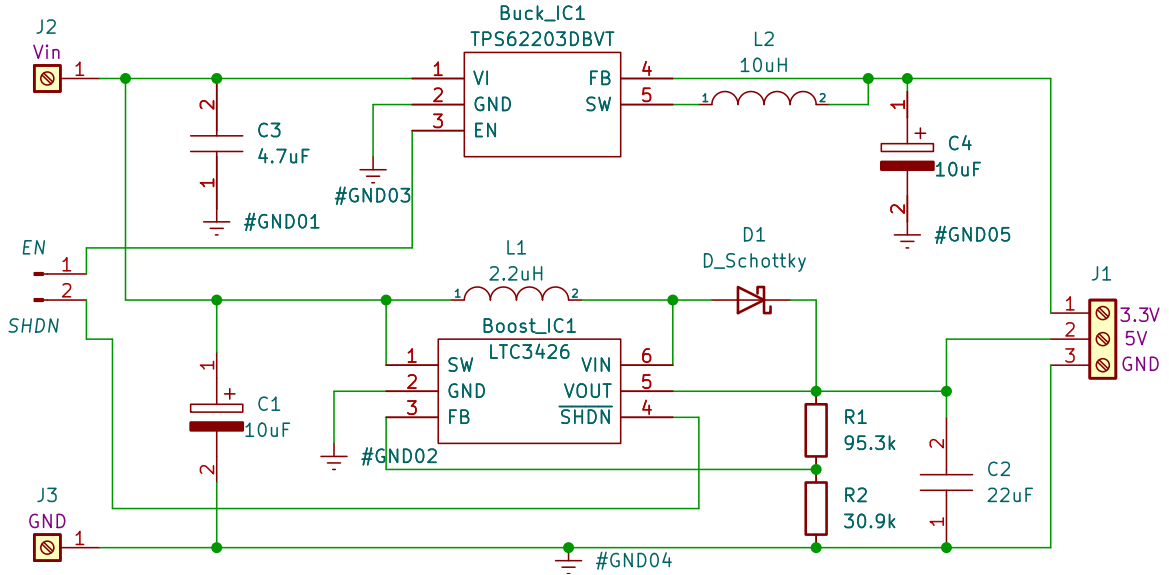


Figure 5.8: LTC3426 as boost IC and TPS62203 as buck IC

5.6 Protection and Measurement Circuits

LTC4361-2 is selected as the over voltage and over current protection IC. It controls an external N-channel MOSFET as a switch to cut the path of current if there is an event of over current or voltage. Manual control of the MOSFET is also possible which may be useful to turn off power to buses by the micro-controller as per different modes of operation of the CubeSat.

Voltage and current passing through each bus and subsystems are continuously monitored by sensors and this information is fed to the micro-controller. These measurements help in estimation of load requirement of subsystems and also help in triggering of protection circuits if a subsystem needs to be turned off in case of an occurrence of a fault.

LTC2990 was chosen as the voltage and current monitor. It can measure the voltage of four external channels and its supply voltage (V_{cc}) simultaneously. It has a 14 bit ADC for measurement. The LTC2990 has the ability to perform 14-bit current measurements with the addition of a current sense resistor. The measurements are passed on to the micro-controller through the two wire I²C interface.

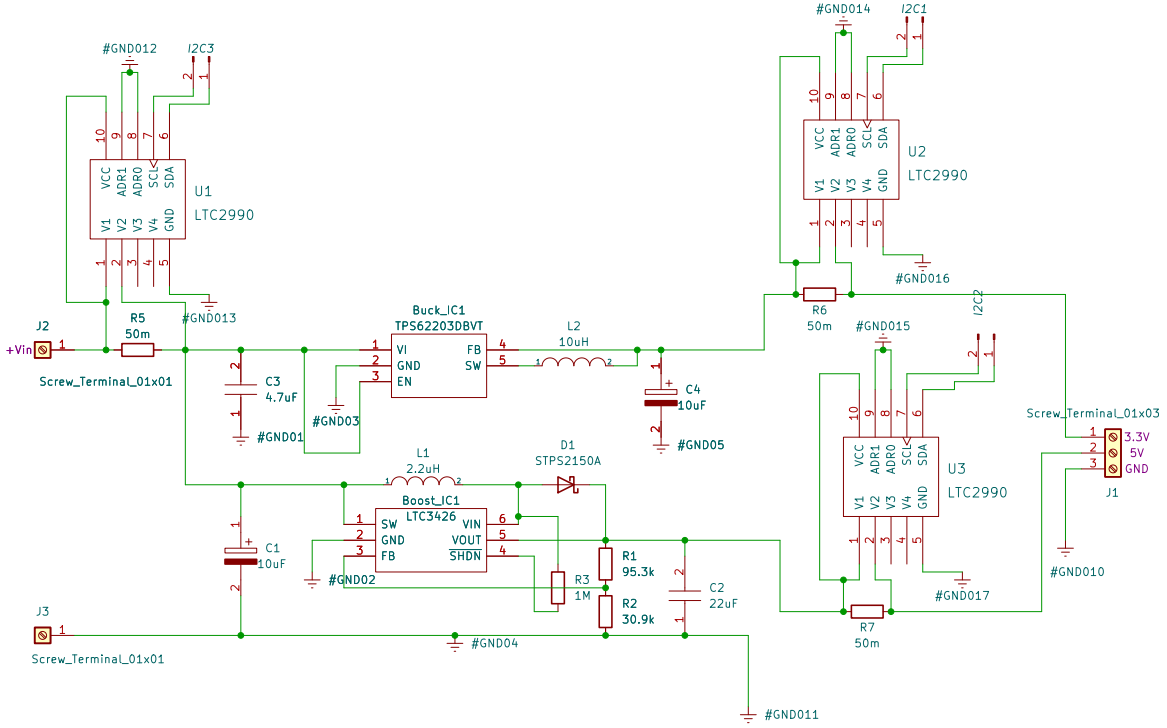


Figure 5.9: Schematic of Buck and Boost circuit with Protection and Voltage and Current Measurement ICs

The screw terminals are used to connect to the power inputs and outputs of the PCB. Pin header connectors are provided for connecting IC control pins to the micro-controller. The pin headers and their functions are given below:

- EN pin of Buck IC: Setting LOW turns off the buck IC
- SHDN pin of Boost IC: Setting LOW turns off the boost IC
- ON1 pin of IC1 (LTC4361): Setting HIGH turns off the MOSFET (IC2 - SI470DH) of the 3.3 V bus
- ON2 pin of IC4 (LTC4361): Setting HIGH turns off the MOSFET (IC3 - SI470DH) of the 5 V bus
- SCLSDA1 pins: I2C connection to micro-controller relaying measured parameters of 3.3 V bus by U2 (LTC2990)

- SCLSDA2 pins: I2C connection to micro-controller relaying measured parameters of 5 V bus by U3 (LTC2990)
- SCLSDA3 pins: I2C connection to micro-controller relaying measured parameters of input bus (V_{in}) by U1 (LTC2990)

5.6.1 PCB Layout

A double layer PCB was designed from the schematic (Ref. Fig. 8.4). The second layer was used as the GROUND plane. The schematic and PCB design was done in KiCad EDA.

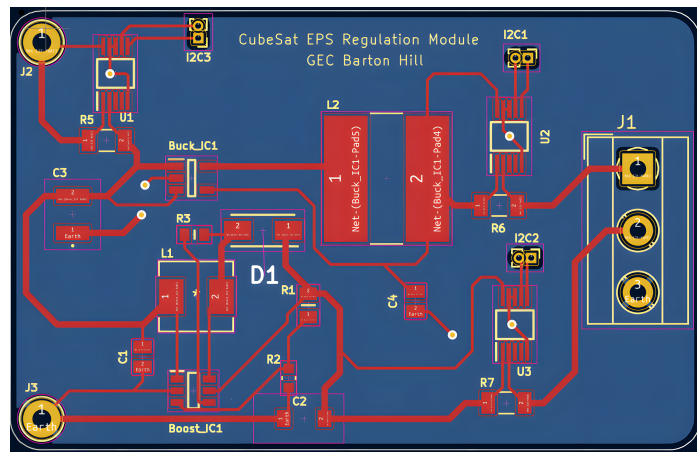


Figure 5.10: Buck and Boost circuit PCB - All Copper Layers only

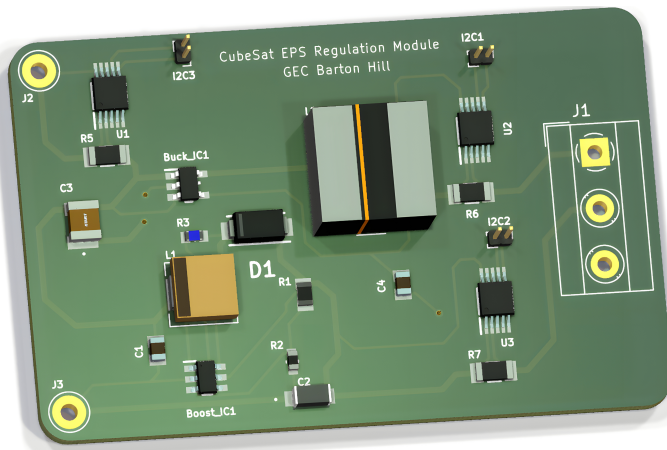


Figure 5.11: Buck and Boost circuit PCB - 3D Model

5.7 Micro-controller

The requirements of micro-controllers depend of the BUS, the other links as digital/analog outputs, the energy consumption, the voltage range and the memory.

The micro-controller has to handle the energy distribution of the entire CubeSat, and has to communicate with the OBC of CubeSat. Thus, it needs digital/analog outputs (for lines going to ADCS, Telemetry, OBC, battery , monitoring IC etc), UART for two-way communication between the micro-controller and the OBC and SPI to send data of the battery level to the micro-controller.

The micro-controller should have low energy consumption, around the micro ampere range for the “Active mode” and around the hundreds of nano ampere for the “Off mode”. It also should need sufficient memory storage to store the readings to provide it to OBC when requested. It should also independently take action during over-current, over voltage happenings, and also should control different power modes of the EPS.

Few considered options were Arduino, Raspberry Pi, TI micro-controllers, STM32 etc. Arduino has limited programming capabilities, and Raspberry Pi was too large for the need and also has high power consumption. STM32 was selected due to its wide range of capabilities, still maintaining the size and power constraints. It also has more community support which makes the programming easier.

STM32 is a ARM Cortex M4 32-bit micro-controller having a flash memory of 512 Kb. It can have upto 81 I/O ports with interrupt capabilities. It can have upto 78 fast I/Os upto 42 MHz, 3 I2C interfaces, 3 USARTs, 4 SPIs etc. We selected STM32401RE development board to test its capabilities, and one of its advantage is that, it can be programmed using Arduino IDE or even MATLAB, apart from its own programming IDE called STM32CUBE IDE.

5.8 Component List

SI No.	Manufacturer Part#	Description	Qty.	Total + GST
1	C1210C475K4RACAUTO	MLCC - SMD/SMT 16V 4.7uF X7R 1210 10% AEC-Q200	4	287.4004211
2	CRCW0603510RJNEA	Thick Film Resistors - SMD 1/10watt 510ohms 5%	10	38.62477875
3	C2012X7R1C105K125AA	MLCC - SMD/SMT 1.0uF 16V 10% 0805	4	78.42567444
4	SI3483DDV-T1-BE3	MOSFET P-CHANNEL 30-V (D-S)	3	175.6558838
5	CRA2512-FZ-R025ELF	Current Sense Resistors - SMD 0.025ohms 1% +/- 50PPM	4	211.8081055
6	SRU1038-100Y	Fixed Inductors 10uH 30% SMD 1038	4	403.418396
7	ERA-1AEB102C	Thin Film Resistors - SMD 0201 1Kohm 0.1% 25ppm	4	185.8752289
8	ERJ-PB6B3002V	Thick Film Resistors - SMD 0805 Anti-Surge Res. 0.1%, 30Kohm	4	178.8937683
9	GRM21BR61C106KE15K	MLCC - SMD/SMT 10uF 16Volts 10%	10	136.0862885
10	ERJ-UP3F1303V	Thick Film Resistors - SMD 0603 Anti-sulfurated anti-surge resistor	4	100.4888077
11	IHLP2020CZER2R2M8A	Power Inductors - SMD 2.2uH 6.6A 26Mohm	4	567.0136108
12	CL03A225KP3CRNC	MLCC - SMD/SMT X5R, 2.2uF, +/-10%, 10v, 0201	10	131.9122925
13	0805YC106KAT2A	MLCC - SMD/SMT 16V 10uF X7R 0805 10%	14	840.496582
14	GRM32ER71A226KE20L	MLCC - SMD/SMT 1210 22uF 10volts X7R 10%	4	309.7570496
15	WSHM2818R0600FEA	Current Sense Resistors - SMD .06ohms 7watt 1%	4	478.3057251
16	CL10A106MP8NNNC	MLCC - SMD/SMT 10uF+/-20% 10V X5R 1 0603	10	74.97750854
17	SRN1060-100M	Power Inductors - SMD 10uH 20% SMD 1060	4	469.5845947
18	C2012COG1H102J060AA	MLCC - SMD/SMT SUGGESTED ALTERNATE 810-C1005C0G1H102J	4	92.91137695
19	WSL2010R1100FEA	Current Sense Resistors - SMD 1/2watt .11ohms 1%	4	295.6332397
20	C1005X8R1C473M050BB	MLCC - SMD/SMT RECOMMENDED ALT 810-C1005X8R1C473K0B	10	80.85810089
21	LTC3426ES6#TRMPBF	Switching Voltage Regulators 1.2 MHz Step-Up DC/DC Converter	4	2723.537598
22	SMM4F5.0A-TR	ESD Suppressors / TVS Diodes 400W HI JCT TMP	2	132.8853455
23	SPV1040T	Battery Management Hi efficiency solar battery charger	4	2022.000854
24	CR0805-FX-9532ELF	Thick Film Resistors - SMD 95.3K 1%	10	33.01148987
25	CMP2512-FX-3903ELF	Thick Film Resistors - SMD ResHighPower 2512 390k 1% 1.5W TC100	4	243.4067993
26	ERJ-S02F2200X	Thick Film Resistors - SMD 0402 220ohms 1% Anti-Sulfur	4	209.5628052
27	WSLP1206R0500FEA	Current Sense Resistors - SMD 1Watt 0.05Ohms 1%	12	589.9055786
28	C3216JB1C226M160AB	MLCC - SMD/SMT RECOMMENDED ALT 810-C3216X5R1C226M	4	291.035675
29	RC0603FR-0730K9L	Thick Film Resistors - SMD 30.9 kOhms 100mW 0603 1%	10	19.37921524
30	IHHP0805ZHER1R0M01	Power Inductors - SMD 0805 1uH 20%	4	216.9559174
Total:				11619.80762

5.9 EPS PCB Design as per PC/104 Specifications

After all the selected components are tested separately and their proper working is ensured, these components can be combined together in a single PCB. This PCB is a four layer PCB with separate 3.3 and 5 V power planes and the bottom layer as the ground plane. A PC/104 connector is used for the ease of stackability of subsystems. As our aim is to design a 1U CubeSat, the PCB dimensions are limited to 9.5 cm x 9.5 cm. For simplifying the design process in KiCad, hierarchical sheets feature was used and the sheets were linked using global labels. The schematics of the different components in the EPS are shown below:

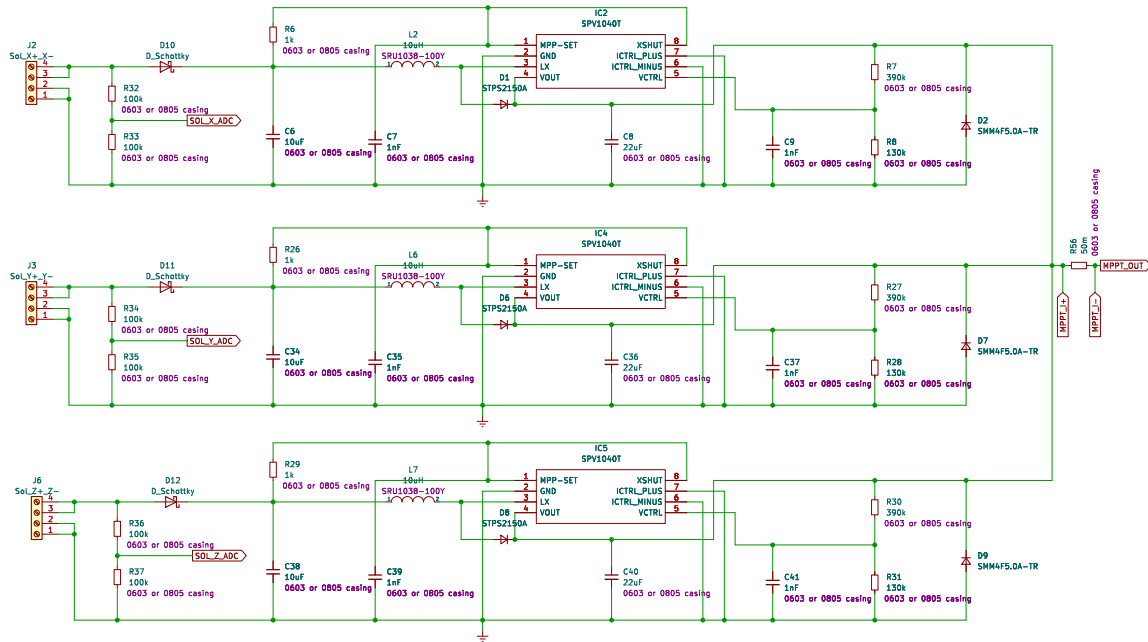


Figure 5.12: MPPT

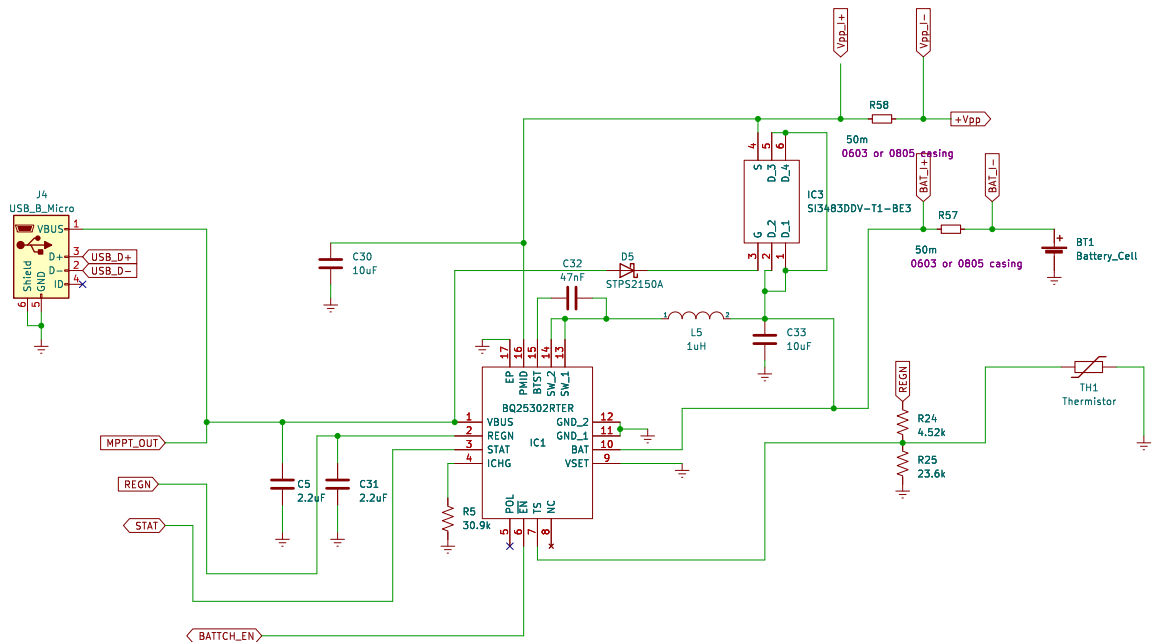


Figure 5.13: Battery Charger

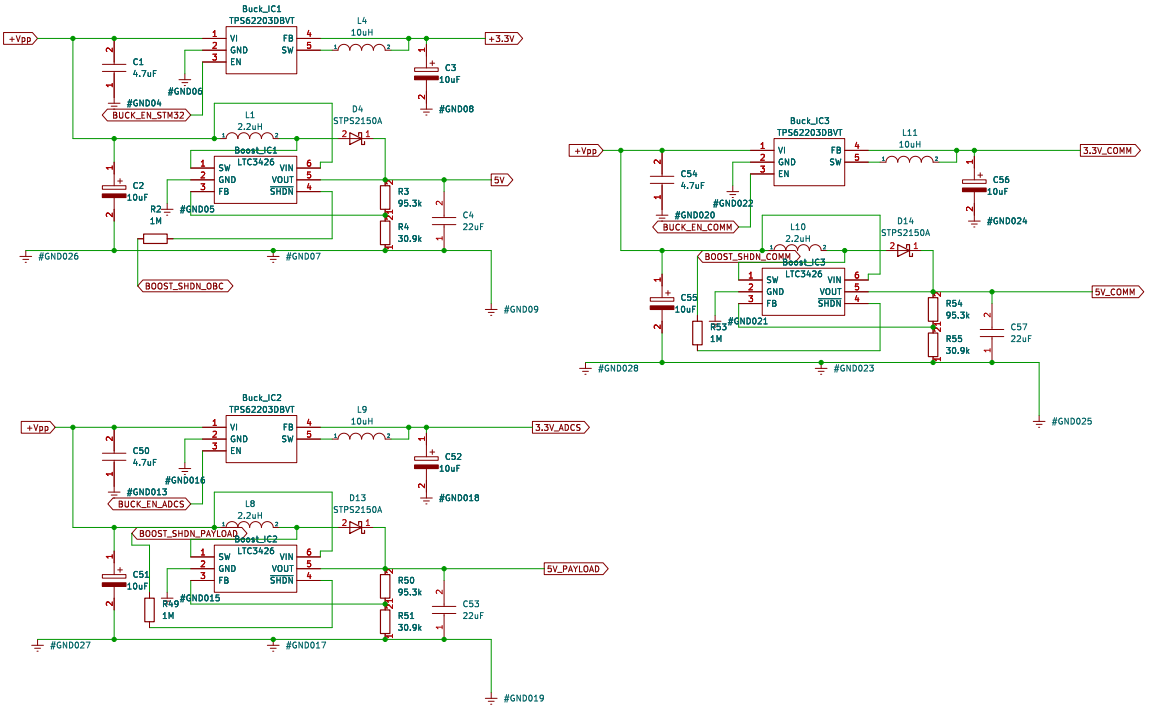


Figure 5.14: Power Regulation circuits

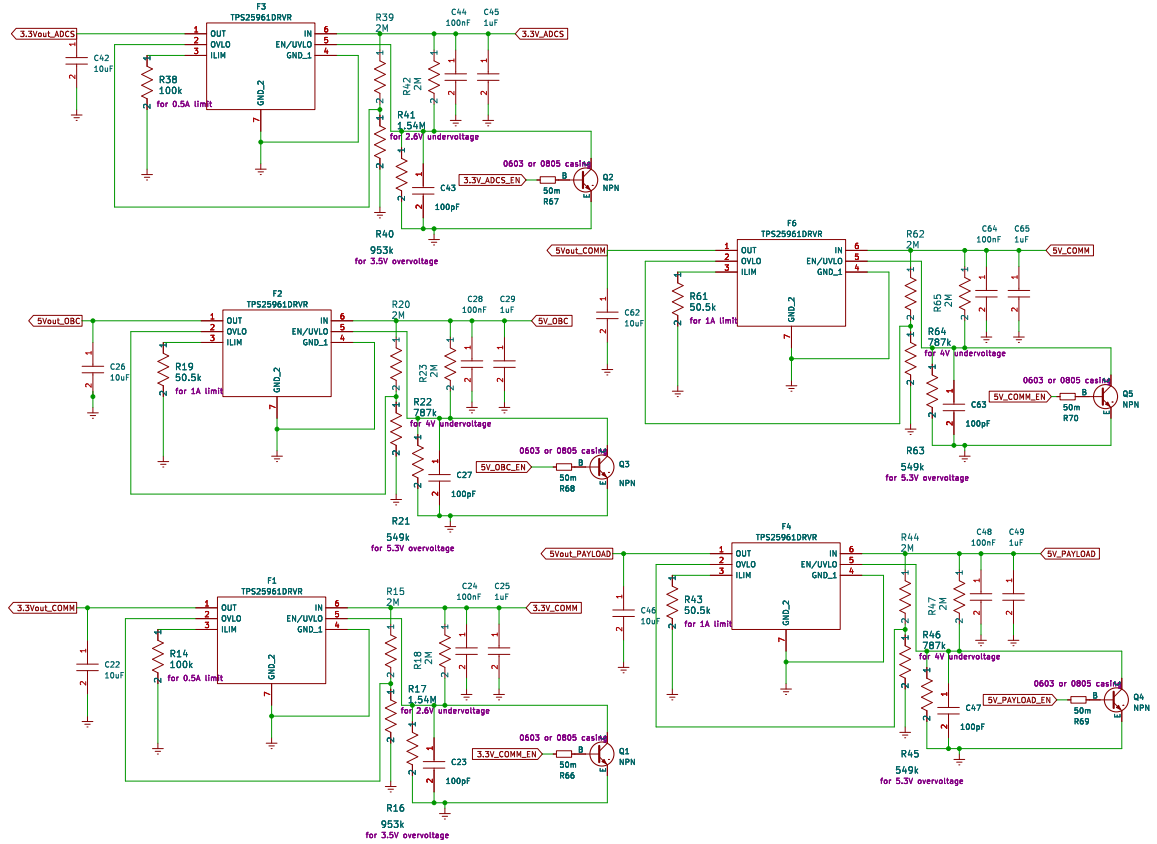


Figure 5.15: Protection eFuse circuits

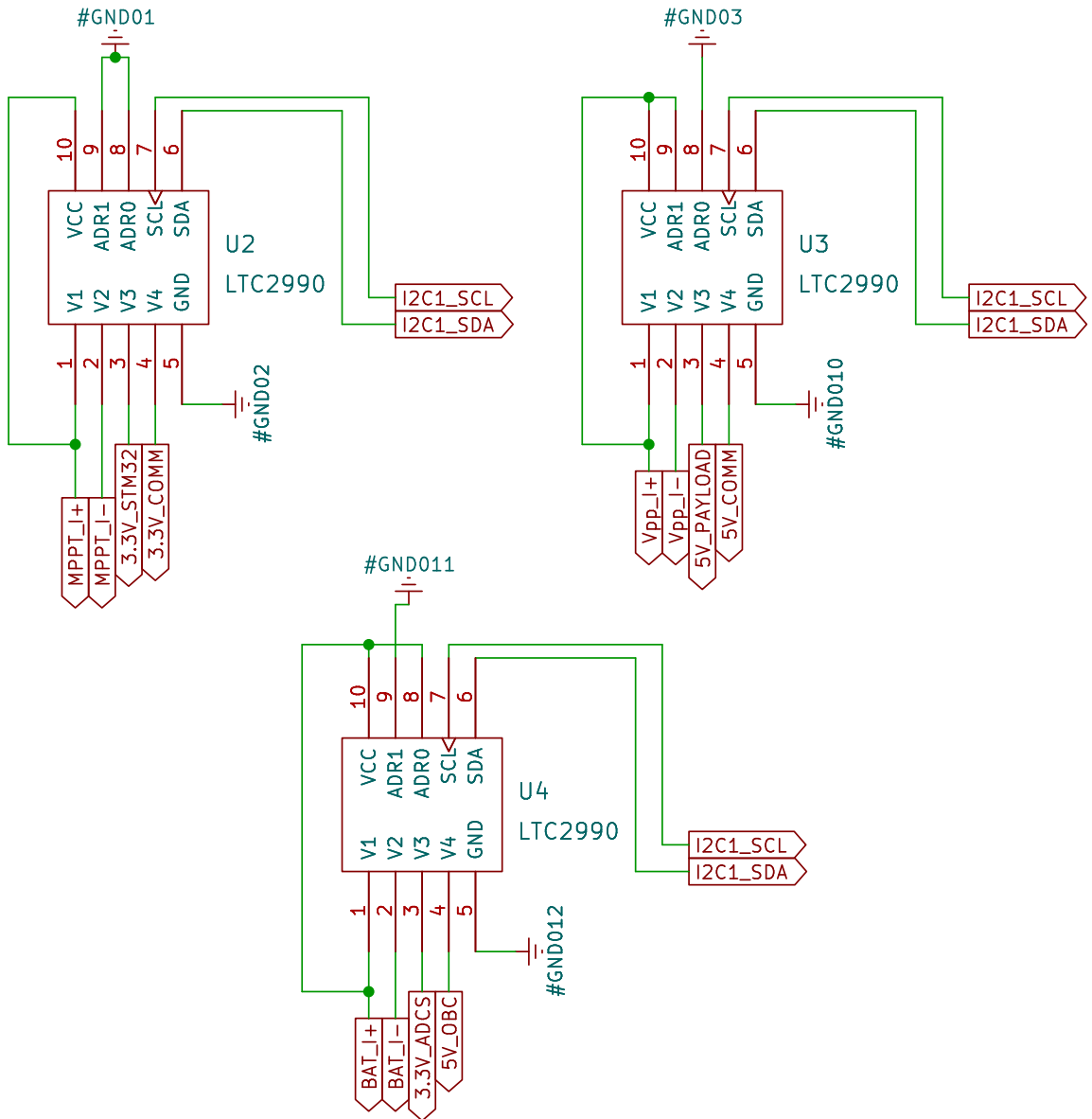


Figure 5.16: Voltage and Current measurement circuits

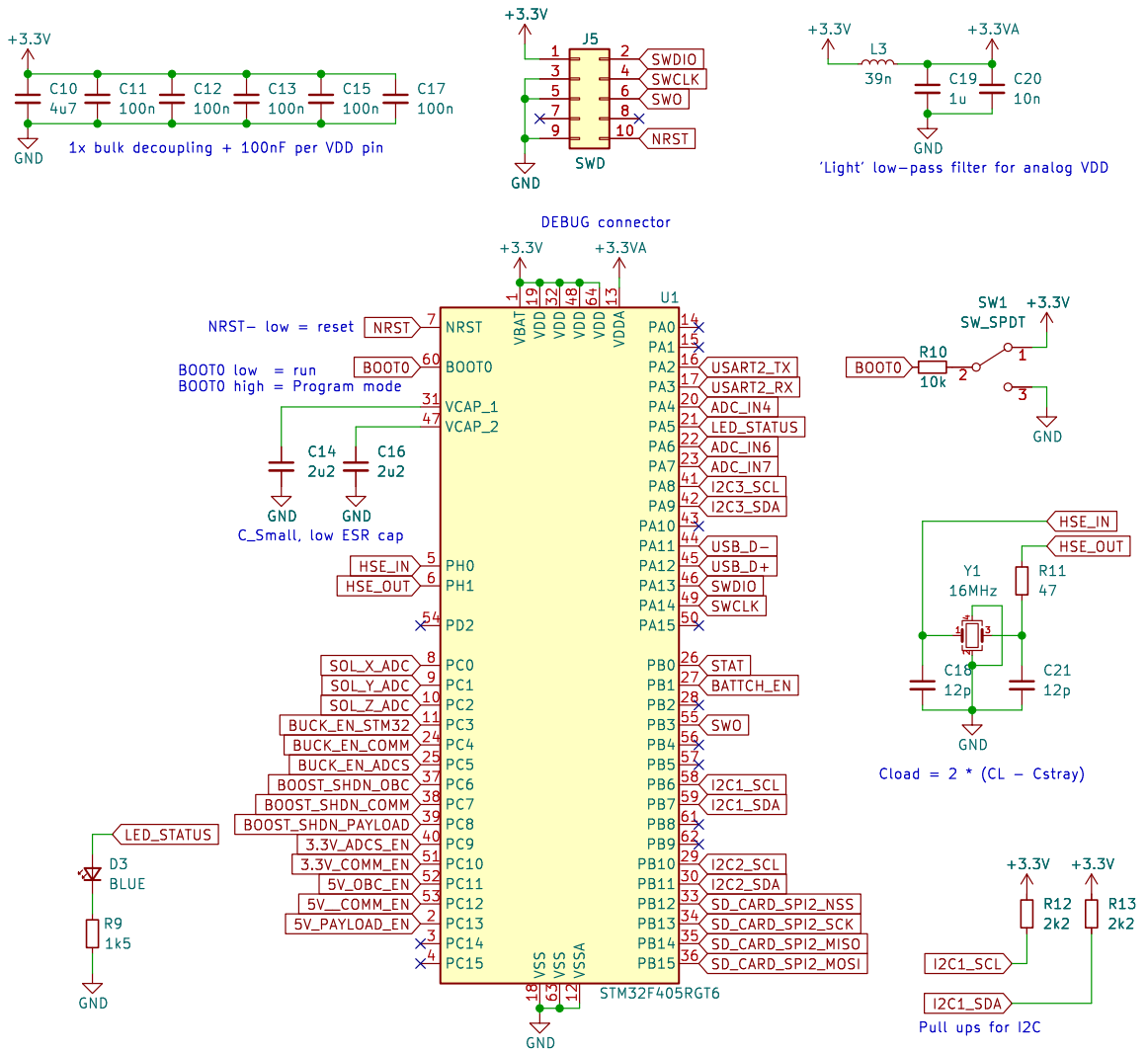


Figure 5.17: STM32 Micro-controller

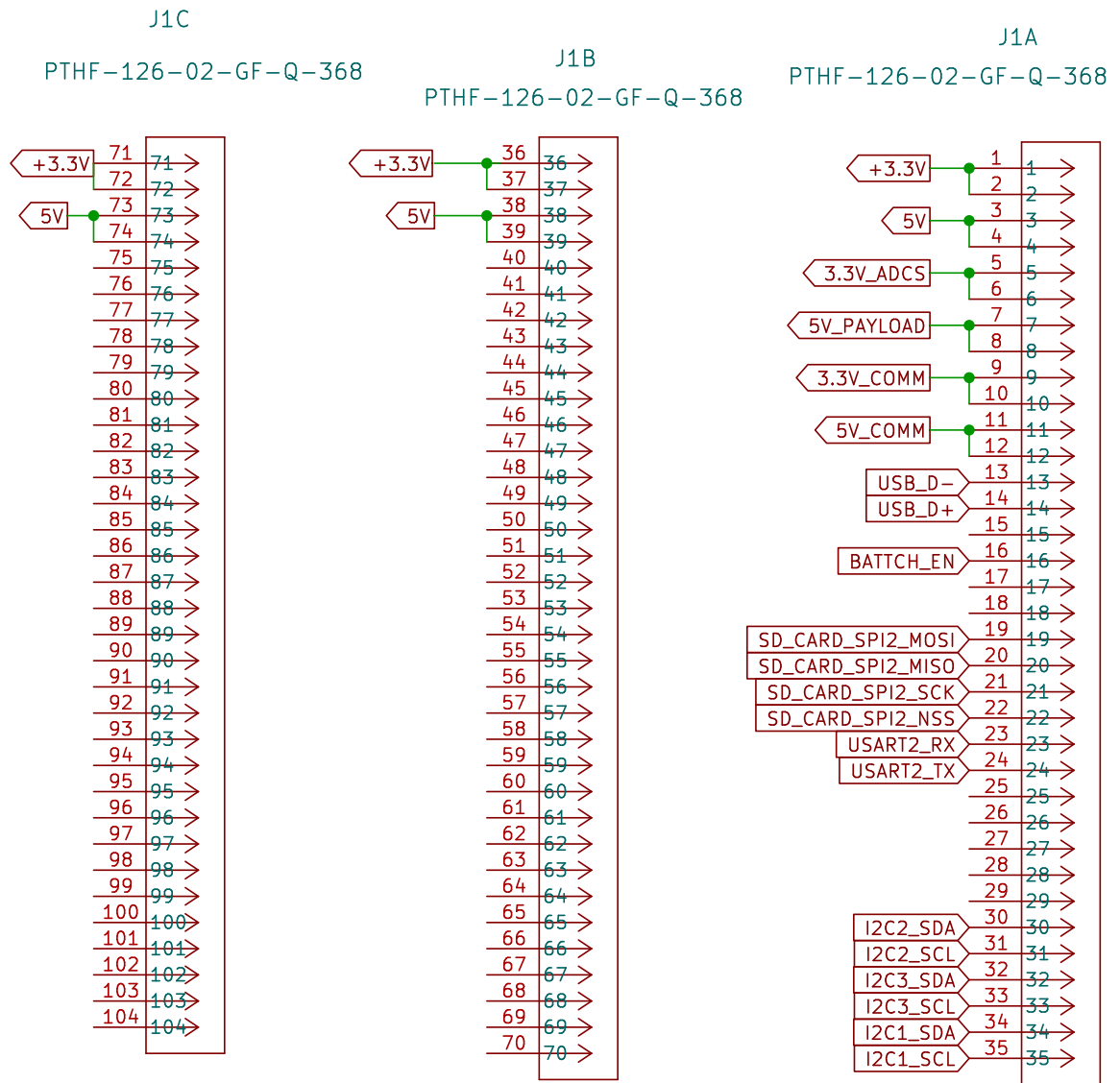


Figure 5.18: PC/104 Connection Pins (Only pins connected to the EPS are labelled)

5.10 3D Model

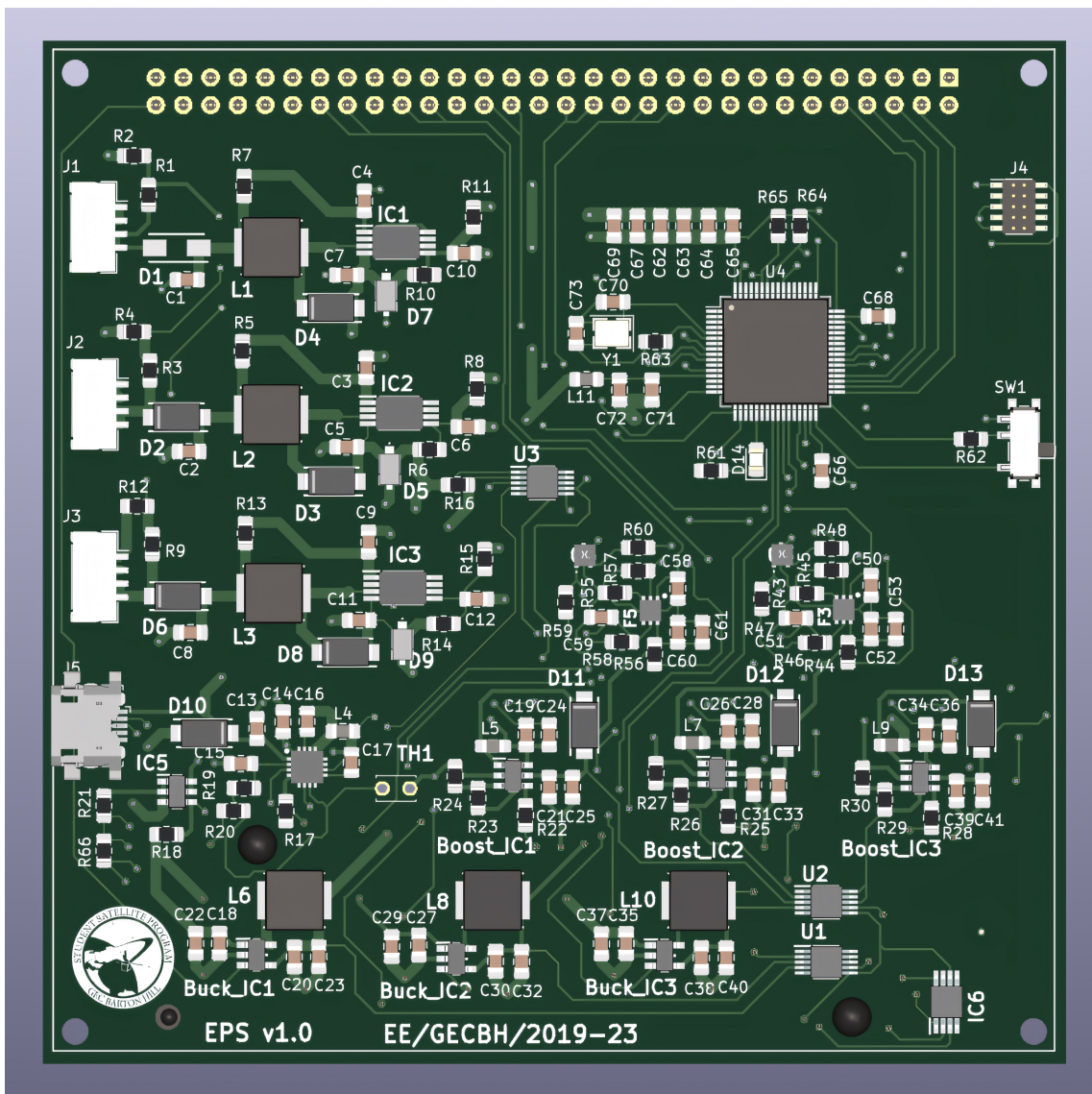


Figure 5.19: 3D Model of EPS PCB (Top Layer)

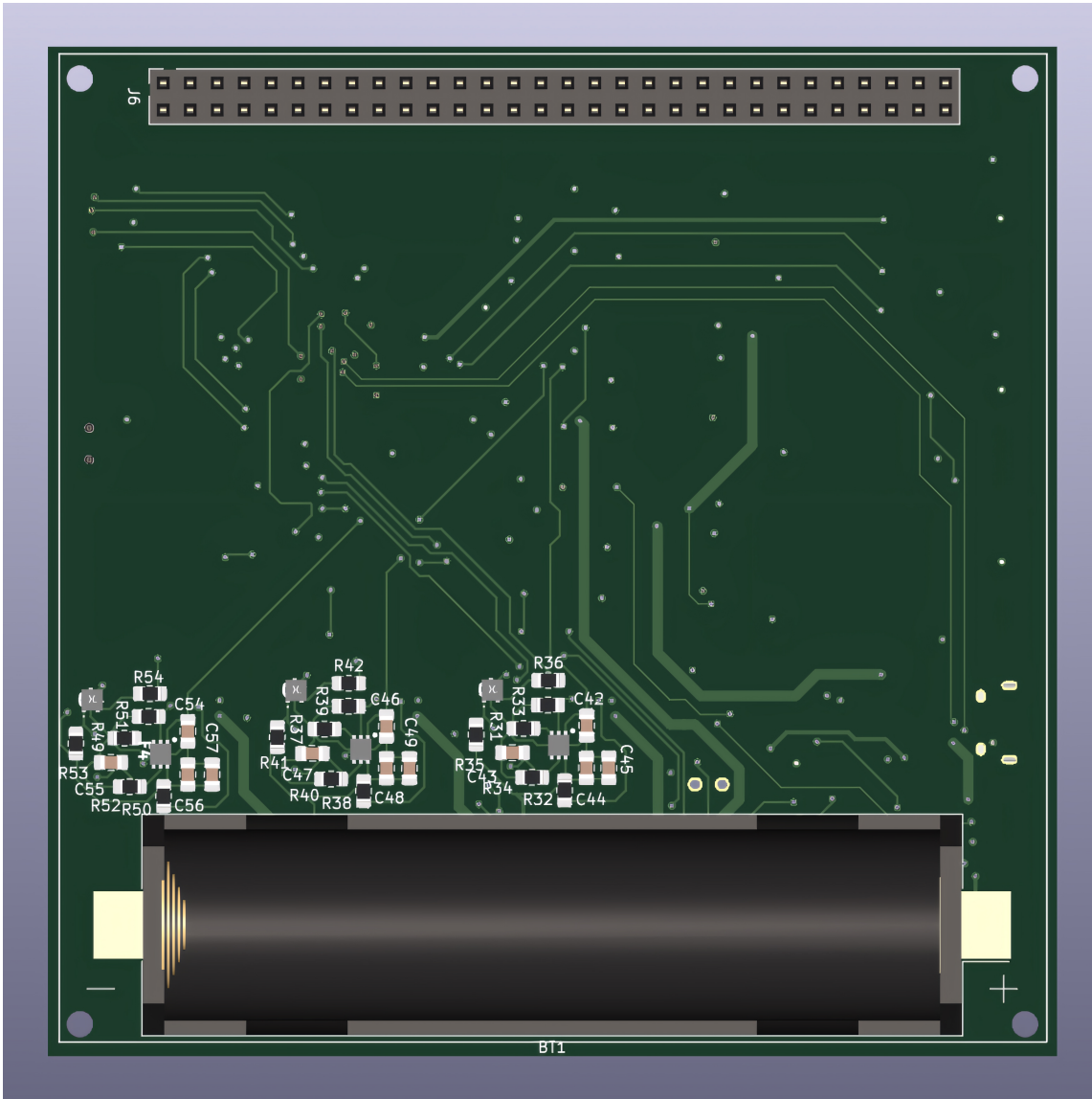


Figure 5.20: 3D Model of EPS PCB (Bottom Layer)

Chapter 6

Testing

6.1 Variable DC load using MOSFET

To test the efficiency of the demo boards, different tests like line regulation, load regulation etc have to be conducted. For line regulation, at a certain constant load, we should create a voltage values table and get the efficiency curve. For that, we need different values of resistance (load). Instead of using resistance, we could use a MOSFET for simulating various load conditions. Since we don't need any higher loads to test the demo boards, a circuit that simulate a load precisely for values from 0 to 2A and with a precision of 0.01A will do the job.

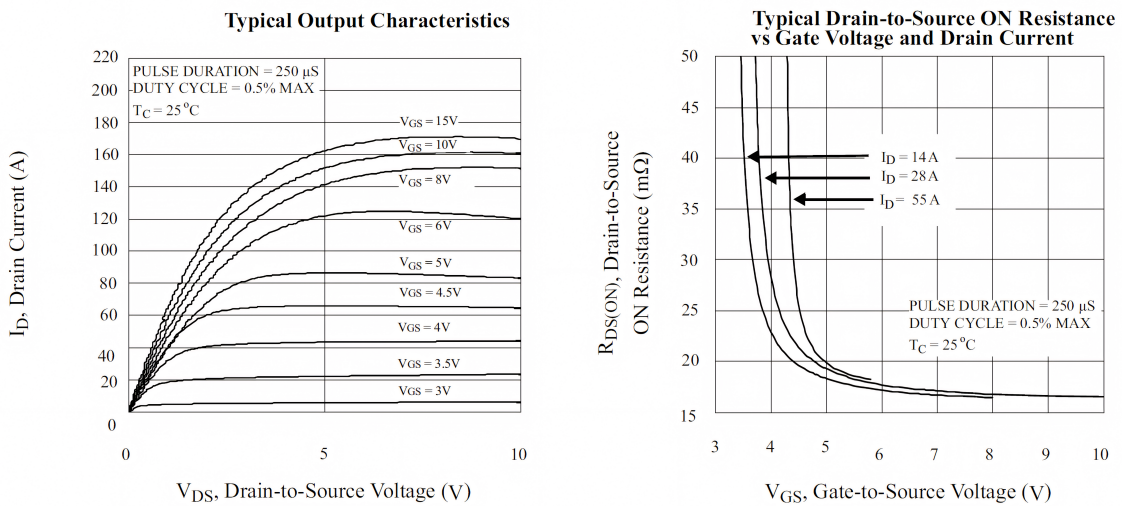


Figure 6.1: Mosfet characteristics

IRFZ44 is the MOSFET used to implement this circuit. It has a V_{ds} on voltage of 10 V. A potentiometer is used to control the gate source voltage and the circuit to be tested is connected between the drain and source terminals. By varying the gate voltage, the drain source conduction can be controlled. The drain source voltage and current increases proportionally with increase in gate voltage and thus the setup acts as a resistive load.

6.2 VirtualBench

The VirtualBench is an instrument which combines a mixed-signal oscilloscope with an arbitrary waveform generator, a digital multi-meter, a programmable DC power supply, and digital I/O. The all-in-one features are simple, convenient, and provide more efficient circuit design, debugging, and validation, and the included software lets us to view all measurements on a single screen.

6.3 Testing of DC/DC converters

DC/DC converters have a specified input voltage operating range. To confirm the DC/DC converter works properly over the entire range of input voltages, they are tested using an adjustable or programmable dc source to provide the input voltage. A dc electronic load is used on the output of the DC/DC converter to set the output load current and simulate the device that the DC/DC converter would power.

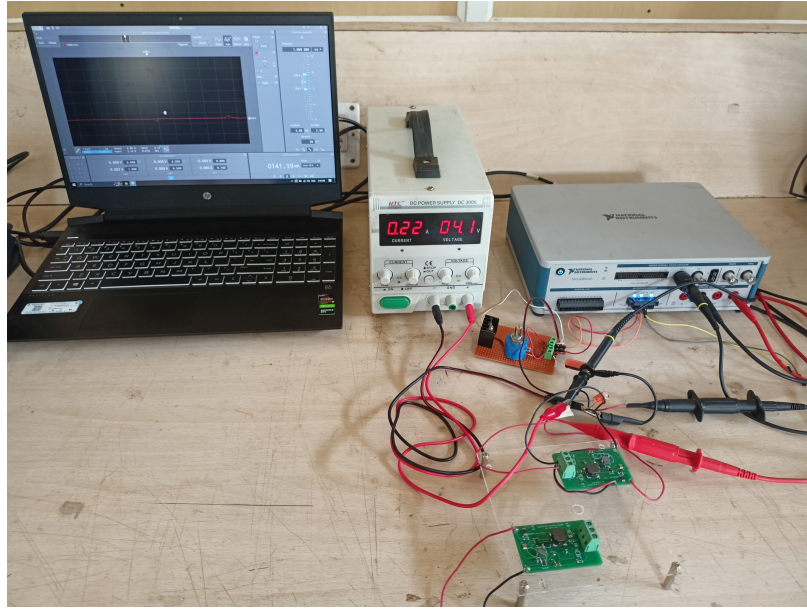


Figure 6.2: Regulation module test setup

6.3.1 Output line regulation

This test confirms that the output voltage stays within specified regulation limits when the input voltage varies from minimum to maximum operating voltage, as defined in the DC/DC converter specification. During this test the output load is usually set to nominal or maximum current as specified.

The output line regulation test involves monitoring the output voltage and recording the total voltage deviation while varying the input voltage from its minimum to maximum specified limits. Some specifications show the output tolerance as a voltage (i.e. 3.3 Vdc \pm 0.02 V) or as a percentage (i.e. 3.3 V \pm 0.5%).

Output regulation R_o is calculated as a percentage and given by the equation:

$$R_o = \left| \frac{V_{omax} - V_{omin}}{V_{onoma}} \right| \times 100$$

where: V_{omax} = Vout at Vin max; V_{omin} = Vout at Vin min; and V_{onoma} = Vout nominal.

Vin (Volt)	Vout (Volt)	Iin (A)	Efficiency
3.6	3.25	0.19	95.02924
4	3.25	0.17	95.58824
4.2	3.21	0.17	89.91597
4.6	3.25	0.16	88.31522
5	3.22	0.15	85.86667
5.5	3.2	0.13	89.51049
6	3.2	0.12	88.88889

Table 6.1: Buck output line regulation at full load (200 mA)

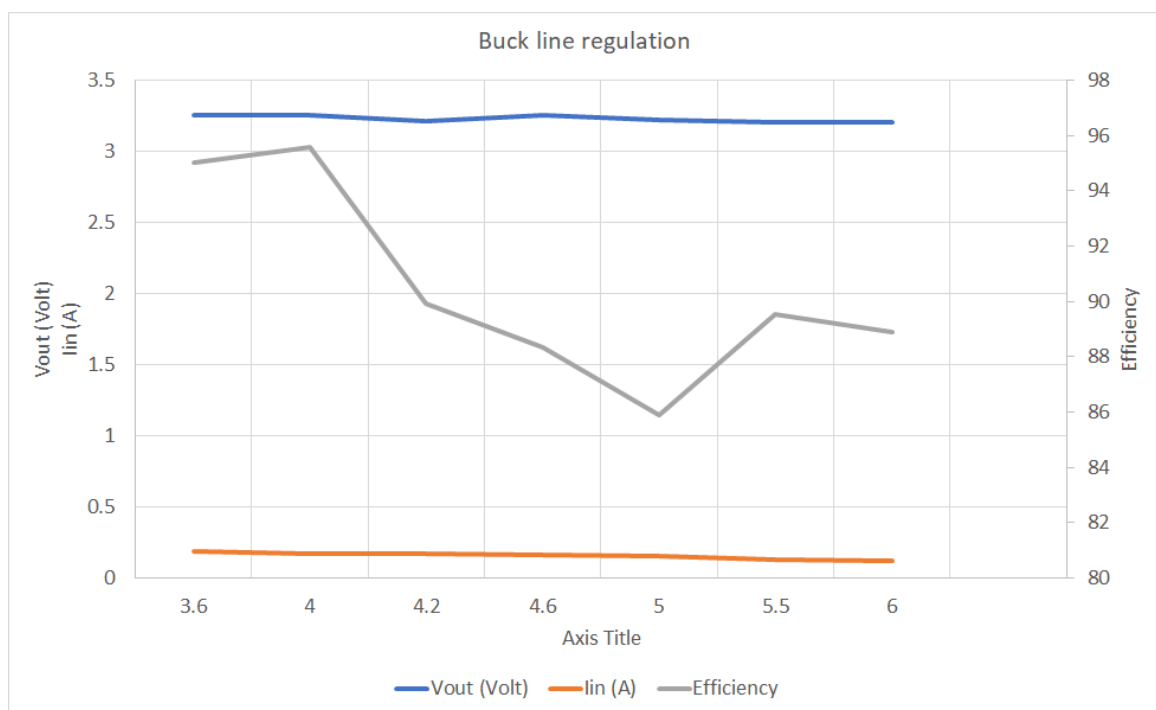


Figure 6.3: Buck output line regulation at full load (200 mA)

Vin (Volt)	Vout (Volt)
3.6	3.3
4	3.35
4.2	3.35
4.6	3.35
5	3.35
5.5	3.35
6	3.35

Table 6.2: Buck output line regulation at no load

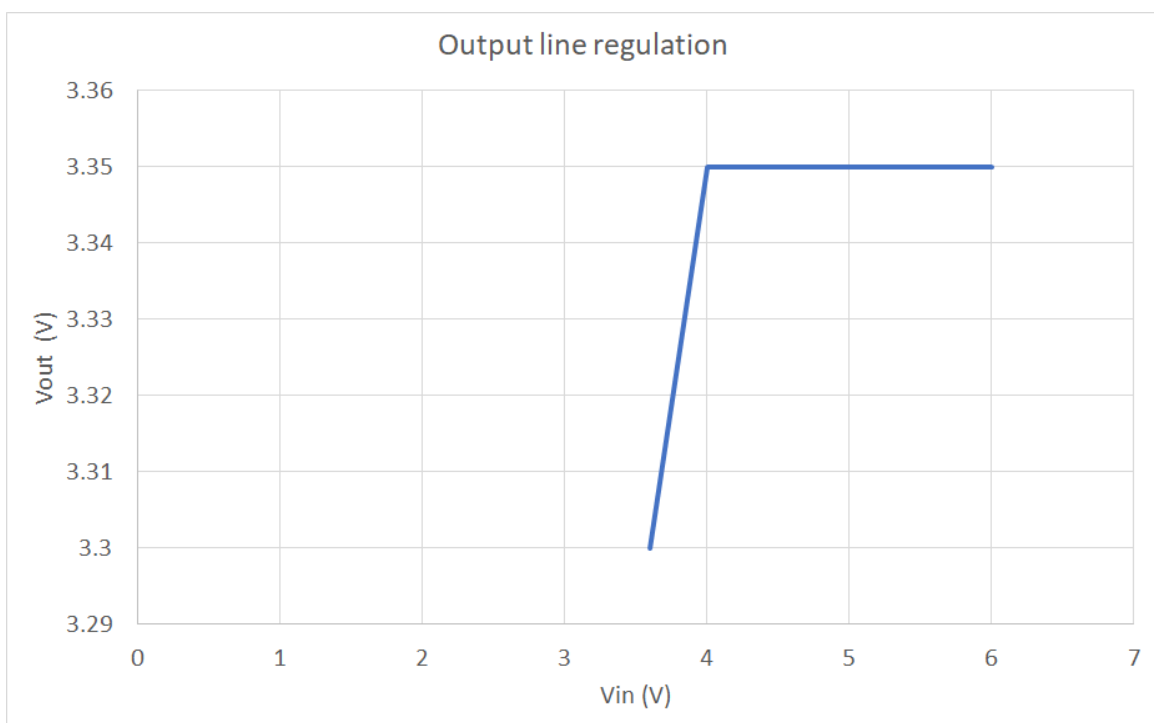


Figure 6.4: Buck output line regulation at no load

Vin (Volt)	Vout (Volt)	Iin (A)	Efficiency
3.6	3.25	0.16	84.63542
4	3.25	0.14	87.05357
4.2	3.26	0.13	89.56044
4.6	3.27	0.12	88.8587
5	3.28	0.11	89.45455
5.5	3.29	0.1	89.72727
6	3.27	0.09	90.83333

Table 6.3: Buck output line regulation at half load(150 mA)

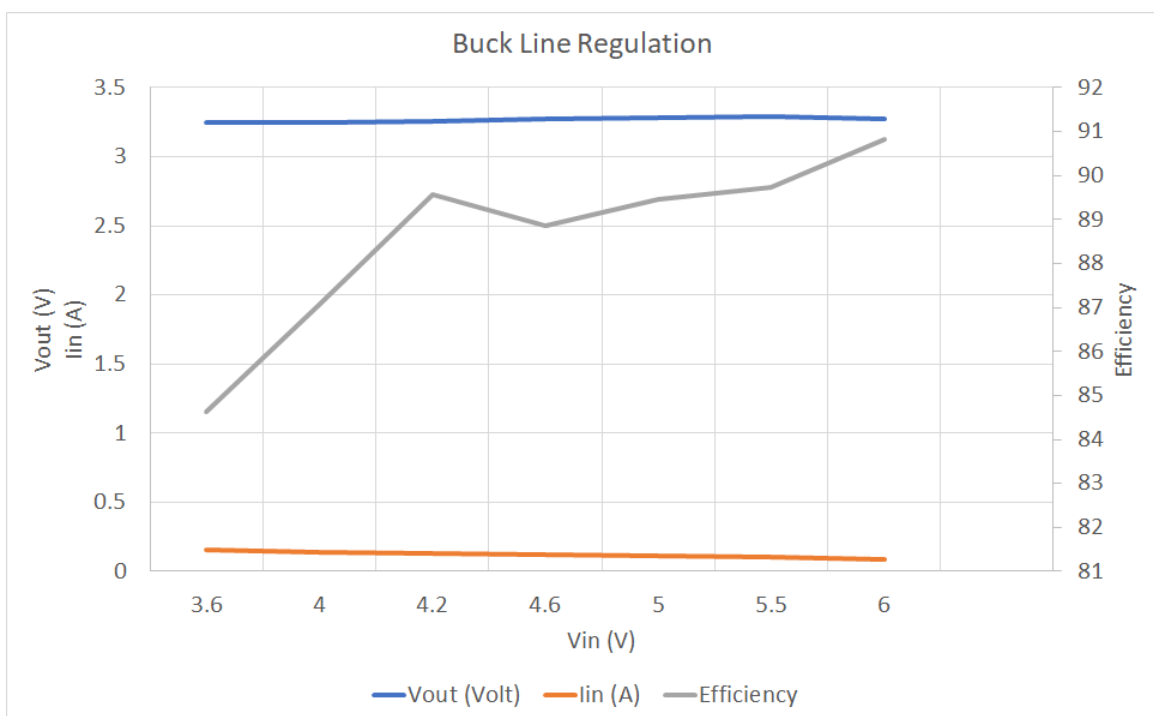


Figure 6.5: Buck output line regulation at half load(150 mA)

Vin (Volt)	Iin (A)	Vout (Volt)	Efficiency
3.6	1.09	3.7	70.71865
4.2	1.24	4.47	64.37212
4.8	1.2	4.8	66.66667

Table 6.4: Boost output line regulation at full load(750mA)

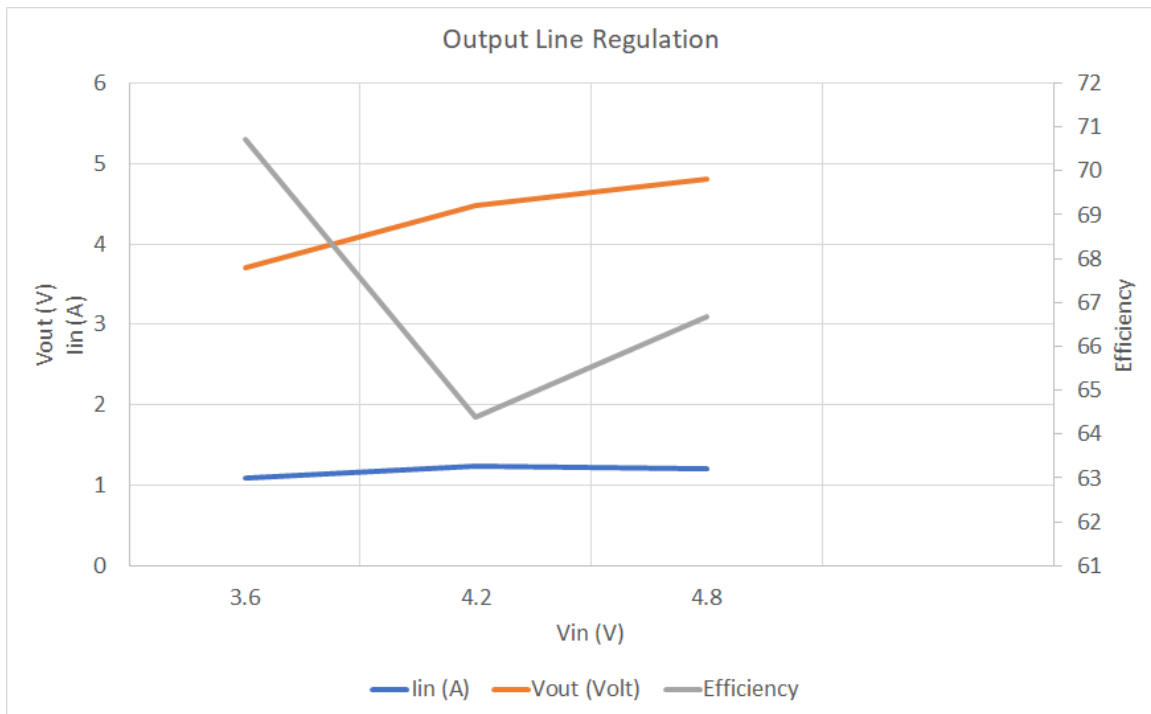


Figure 6.6: Boost output line regulation at full load (750 mA)

Vin (Volt)	Iin (A)	Vout (Volt)	Efficiency
3.3	0.84	4.93	71.13997
4.2	0.68	5.13	71.84874
5	0.65	5.05	62.15385

Table 6.5: Boost output line regulation at half load(400 mA)

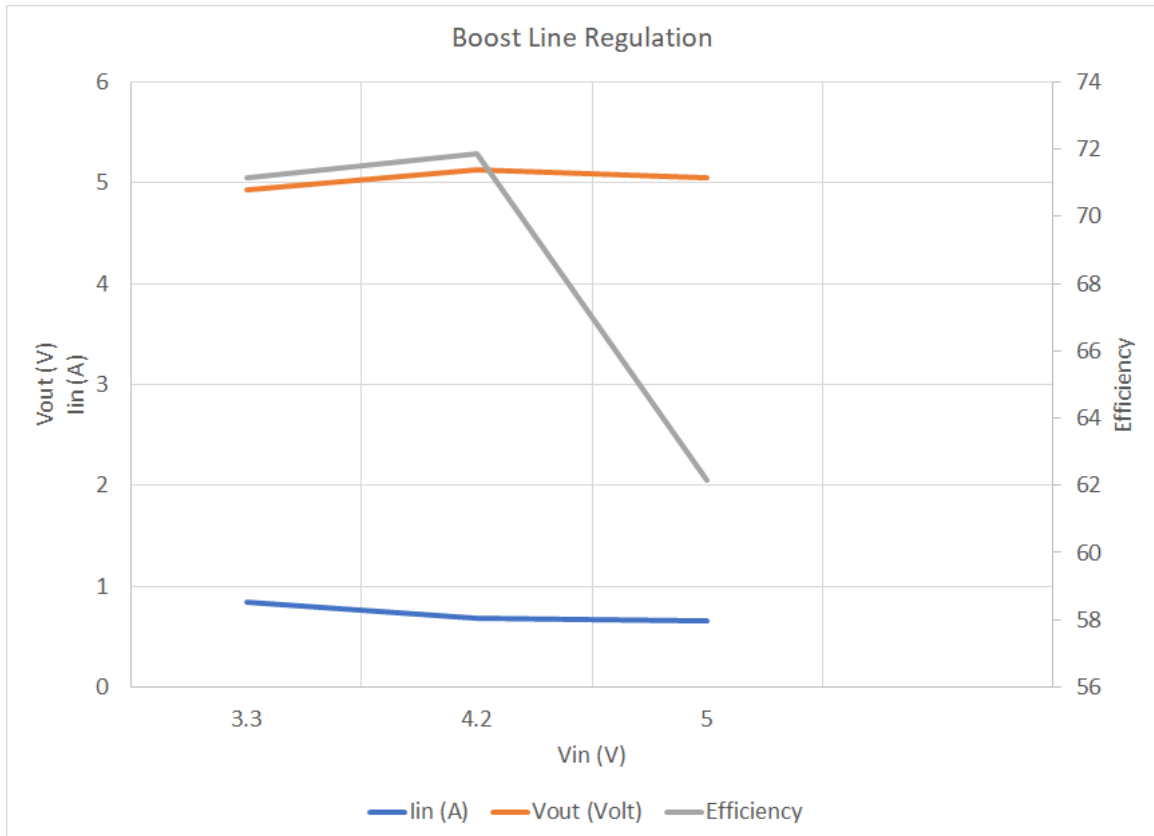


Figure 6.7: Boost output line regulation at half load (400 mA)

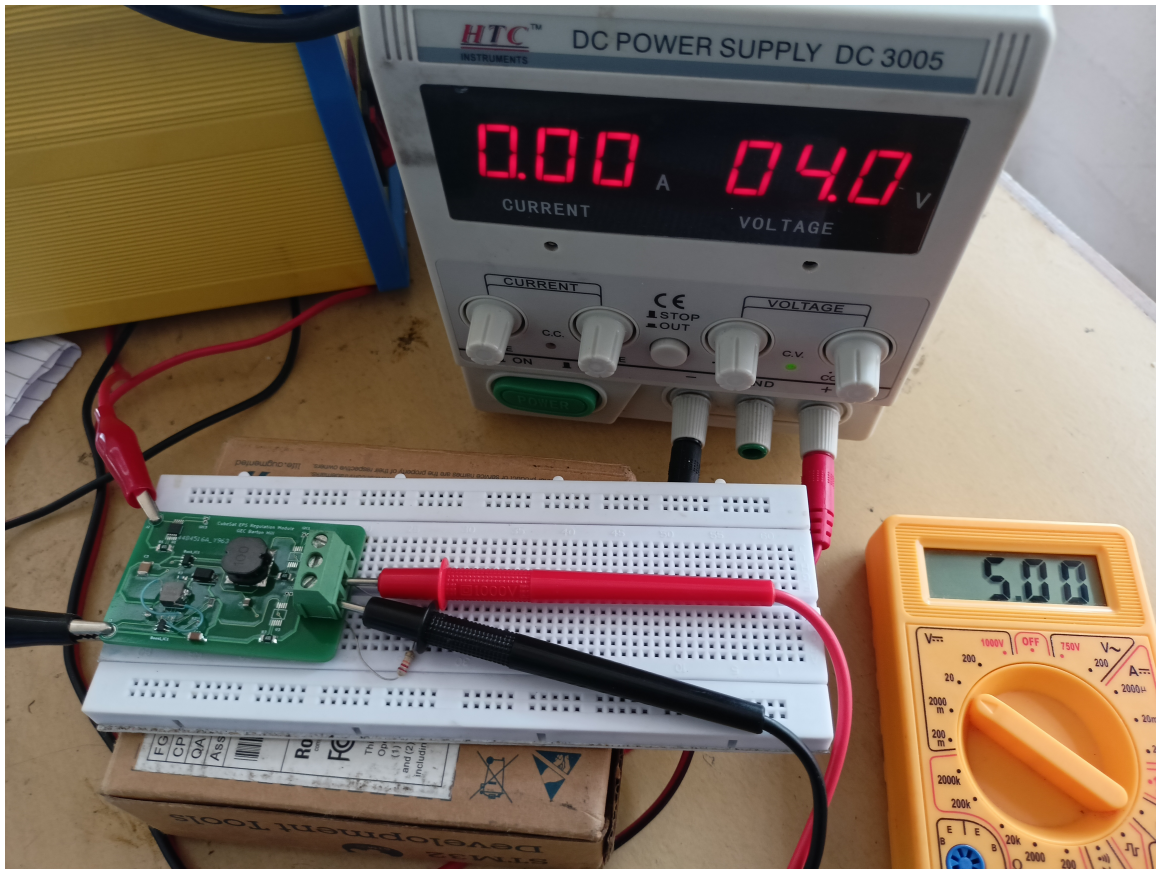


Figure 6.8: Testing of boost converter in 5 V rail

6.3.2 Output load regulation

The output load regulation test ensures the DC/DC converter output voltage stays within the specified regulation tolerance. Here, the change in output voltage is recorded while load is varied from minimum to maximum current. This delta voltage is used to calculate the percentage of deviation which is compared to the specified load regulation limits. Load regulation L_r is calculated as a percentage from the equation:

$$L_r = \left| \frac{V_{oio} - V_{oim}}{V_{onom}} \right| \times 100$$

Where: V_{oio} = Vout at Iout max; V_{oim} = Vout at Iout min; and V_{onom} = Vout nominal.

Iout (mA)	Vout (Volt)	Iin(A)	Efficiency
50	4.94	0.09	76.23457
100	4.94	0.18	76.23457
150	4.91	0.28	73.06548
200	4.89	0.39	69.65812
250	4.87	0.49	69.01927
300	4.87	0.61	66.53005
350	4.87	0.77	61.4899
400	4.86	0.86	62.7907
450	4.7	0.99	59.34343
500	4.44	0.92	67.02899
550	4.6	1.01	69.58196

Table 6.6: Boost load regulation at 3.6 V Vin

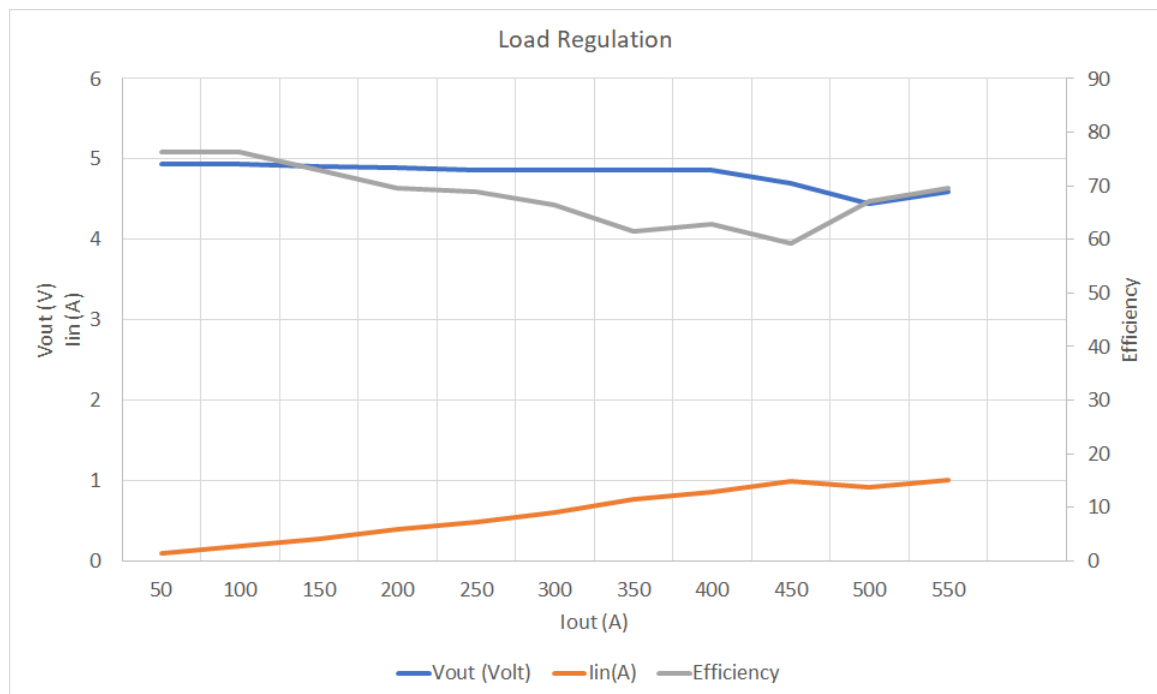


Figure 6.9: Boost load regulation at 3.6 V Vin

Iout (mA)	Vout (Volt)	Iin(A)	Efficiency
50	4.94	0.07	84.01361
100	4.93	0.15	78.25397
150	4.9	0.2	87.5
200	4.87	0.31	74.80799
250	4.87	0.39	74.32845
300	4.86	0.47	73.86018
350	4.86	0.57	71.05263
400	4.86	0.66	70.12987
450	4.85	0.76	68.37406
500	4.84	0.87	66.22879
550	4.81	0.96	65.6126
600	4.76	1.07	63.5514
650	4.62	1.13	63.27434
700	4.45	1.19	62.32493
750	4.38	1.21	64.63991
800	4.1	1.26	61.98035

Table 6.7: Boost load regulation at 4.2 V Vin

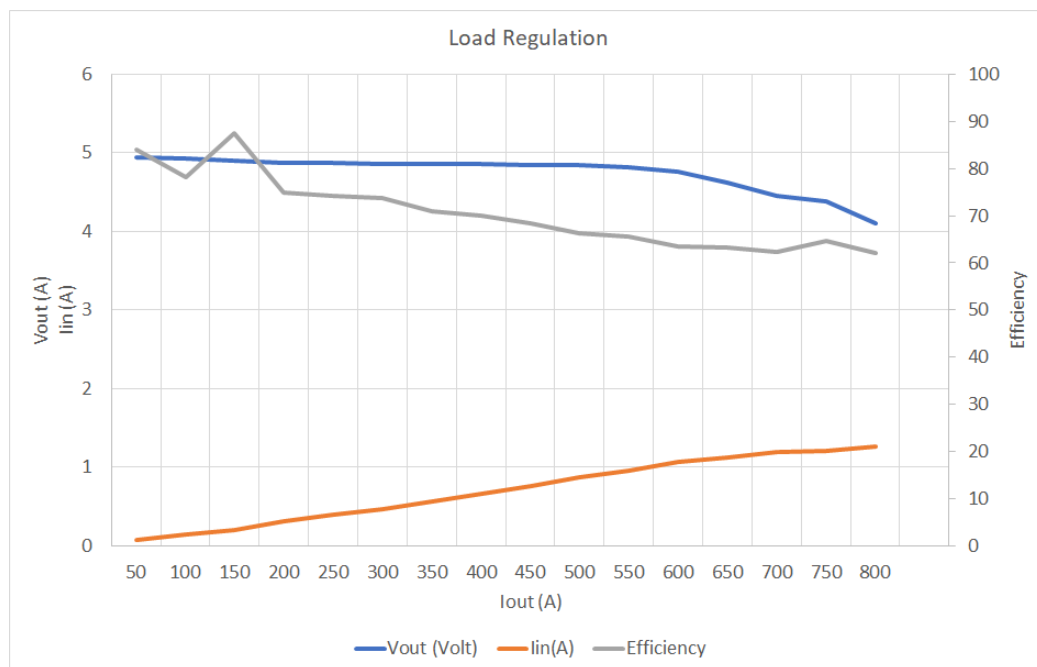


Figure 6.10: Boost load regulation at 4.2 V Vin

Iout (mA)	Vout (Volt)	Iin(A)	Efficiency
100	4.93	0.12	82.16667
200	4.87	0.25	77.92
300	4.86	0.39	74.76923
400	4.84	0.54	71.7037
500	5.02	0.66	76.06061
600	5.02	0.85	70.87059
700	5.02	1.01	69.58416
800	5.02	1.19	67.4958

Table 6.8: Boost load regulation at 5.0 V Vin

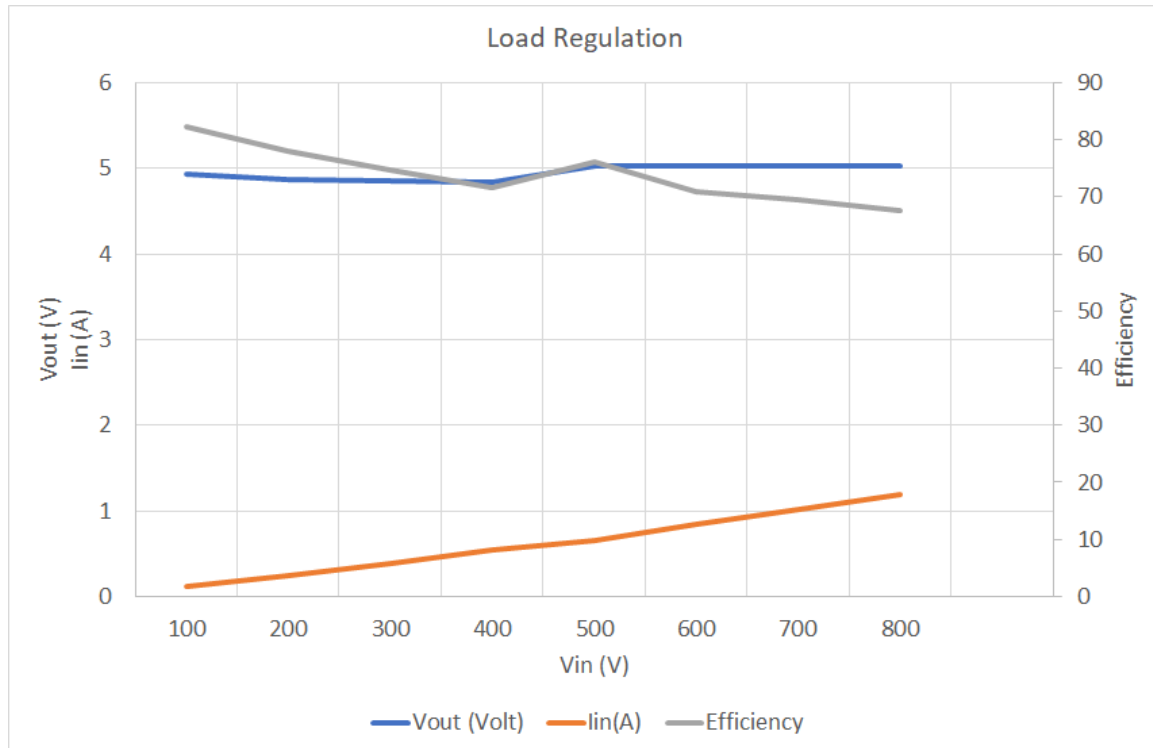


Figure 6.11: Boost load regulation at 5.0 V Vin

Iout (mA)	Vout (Volt)	Iin (A)	Efficiency
50	3.32	0.06	76.85185
100	3.28	0.11	82.82828
150	3.28	0.16	85.41667
200	3.27	0.21	86.50794
250	3.2	0.27	82.30453
300	3.22	0.32	83.85417
350	3.21	0.38	82.12719

Table 6.9: Buck load regulation at 3.6 V input

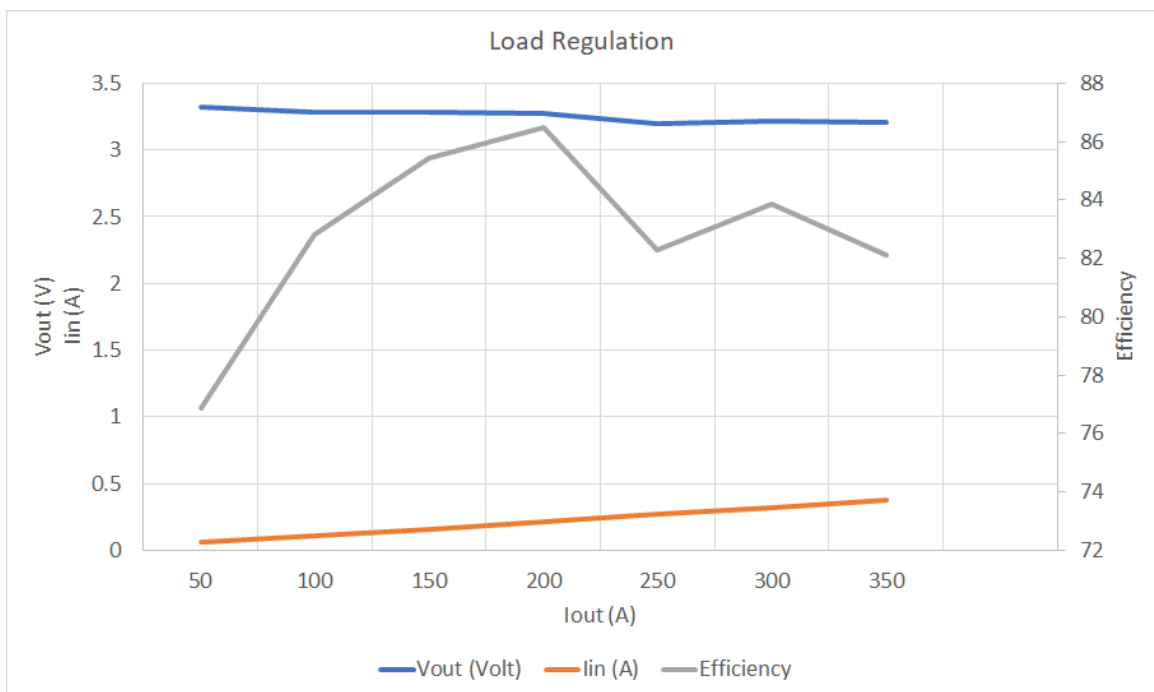


Figure 6.12: Buck load regulation at 3.6 V input

Iout (mA)	Vout (Volt)	Iin (A)	Efficiency
50	3.24	0.04	84.375
100	3.23	0.08	84.11458
150	3.23	0.12	84.11458
200	3.21	0.16	83.59375
250	3.21	0.21	79.6131
300	3.22	0.25	80.5
350	3.18	0.27	85.87963

Table 6.10: Buck load regulation at 4.8 V input

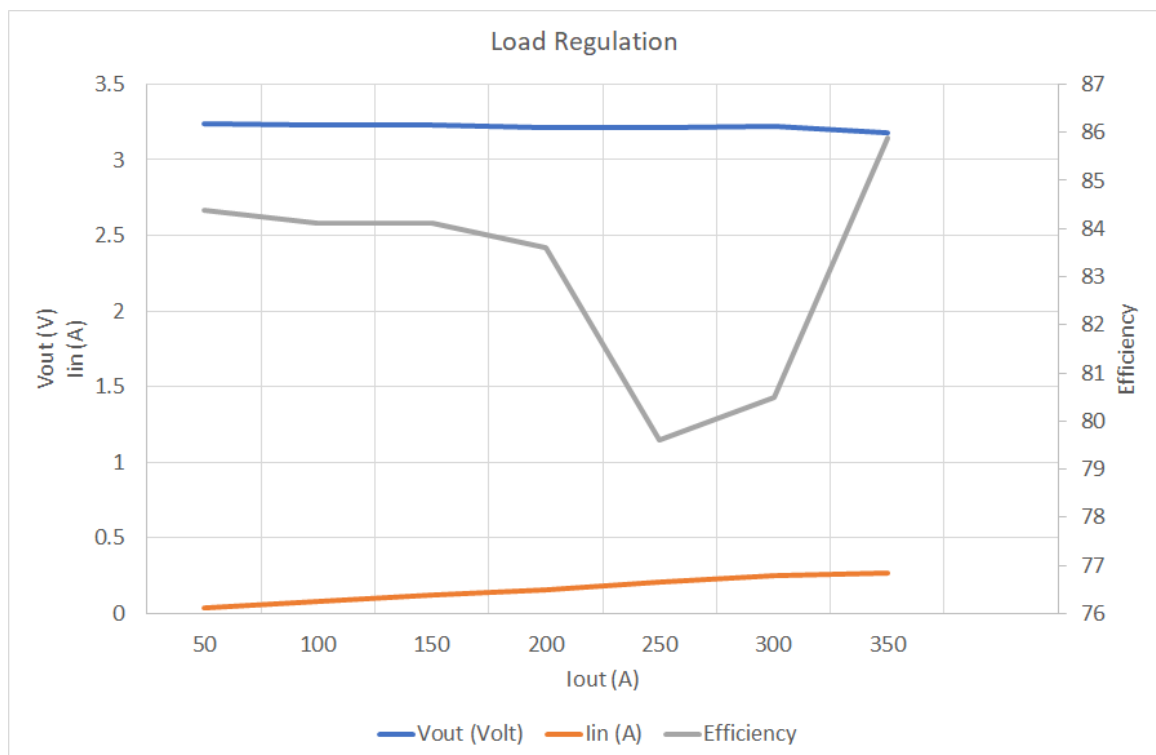


Figure 6.13: Buck load regulation at 4.8 V input

Iout (mA)	Vout (Volt)	In (A)	Efficiency
50	3.3	0.03	91.66667
100	3.21	0.06	89.16667
150	3.26	0.1	81.5
200	3.21	0.13	82.30769
250	3.22	0.15	89.44444

Table 6.11: Buck load regulation at 6 V input

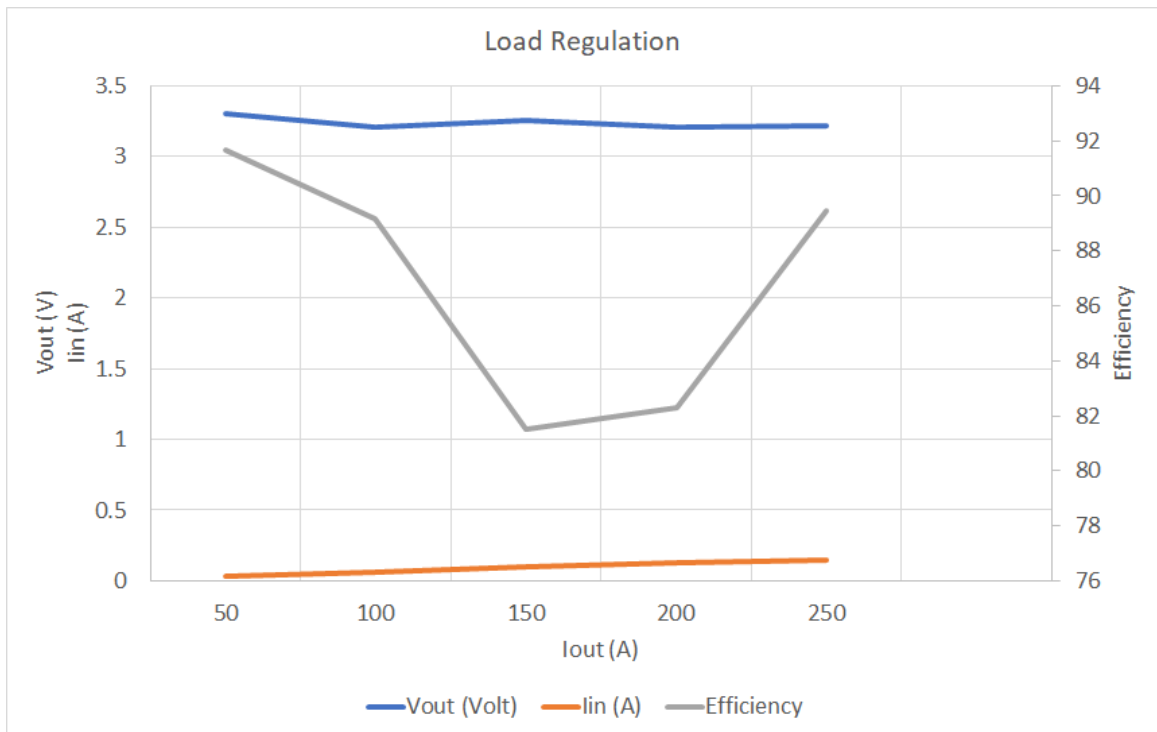


Figure 6.14: Buck load regulation at 6 V input

6.3.3 Output over-current protection

The output over-current protection is intended to protect the DC/DC converter and the device it powers when the load exceeds the converter's maximum rated current. There are different methods used in over-current protection. But the typical approaches are fold-back current limit and pulsing current-limit. The latter is generally referred to as hiccup-mode current limit.

Here are the differences between the two methods: In fold-back current limiting, the output voltage begins to drop and limits the output current supplied to the load as the load current rises above the current-limit set point. In hiccup current limiting, the output turns off when the output current exceeds the rated current limit point. It eventually turns back on. If the load continues to exceed the current-limit set-point, the output will continue turning on and off, hence the hiccup-mode name.

6.3.4 Output over-voltage protection

Most DC/DC converters have a built-in protection circuit that will shut off the output of the device when the output voltage is detected to be over the maximum limit. This facility is referred to as over-voltage protection (OVP). This protects the DC/DC converter from external excessive voltage applied to the converter output. If the DC/DC converter has an adjustable output (trimmed or programmable output voltage), it may be possible to increase the output voltage until the OVP point is exceeded and the protection circuit activates.

If the DC/DC converter does not have an adjustable output, an external voltage source can be applied across the output terminal, increased to the OVP trip point, then removed to see if the output has triggered and turned off.

DC/DC converters having an OVP fault signal can use it to determine if the output detected the OVP and, if so, shut off the output. The output voltage is monitored to determine when the OVP happened and then compared to the OVP specified limits.

6.3.5 Efficiency

Efficiency determines the internal power dissipated by the DC/DC converter and how efficiently input power transfers to the converter output. This test usually

takes place at the nominal input voltage and with the output load set to nominal or maximum specified ratings. The input voltage, current, and power is measured while the same parameters are measured on the output. Efficiency percentage E_p comes from the equation:

$$E_p = \left| \frac{V_{out} - I_{out}}{V_{in} - I_{in}} \right| \times 100$$

where: V_{out} and I_{out} = converter output voltage and current; V_{in} and I_{in} = converter input voltage and current.

This test can also capture the efficiency at various power levels. It's common to plot the data to show efficiency versus output-current.

6.4 Battery Charger Testing

The battery charger IC selected was BQ25302 which is a Li-ion constant current - constant voltage (CCCV) charger. With the constant current function pumping current into the battery, its voltage obviously rises. And as soon as it reaches the set charging voltage of the IC the current falls underneath the constant current limit and thus it enters the constant voltage mode at which point the battery charges up to its max capacity where almost no current is flowing any more. This method is used to prevent overcharging of batteries.

In this circuit, the charging voltage was set at 4.2 V as per the data-sheet of the battery. From fig. 6.16, it is clear that the battery charges in constant current mode and its voltage rises to approximately 4.2 V. Then the charger switches to constant voltage mode and the charging current reduces to zero eventually.

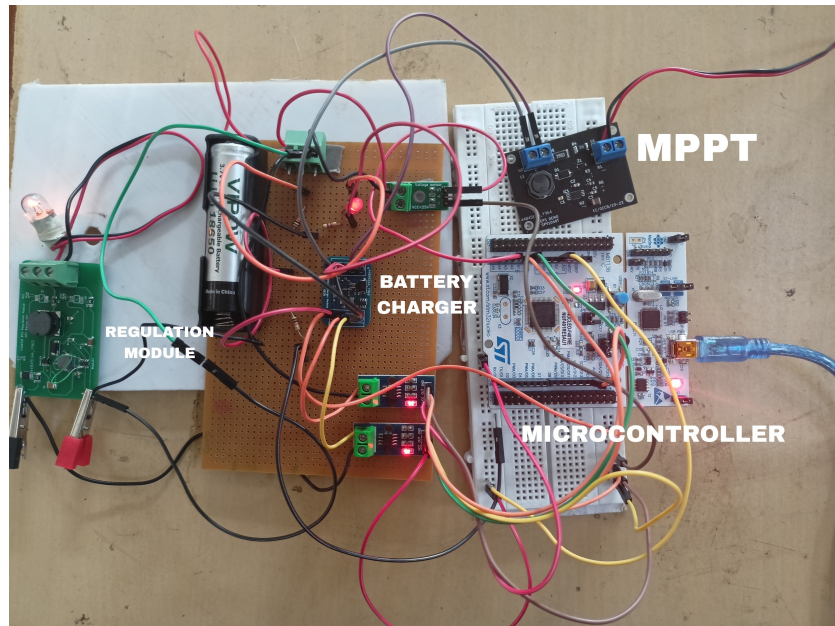


Figure 6.15: Battery charger test setup

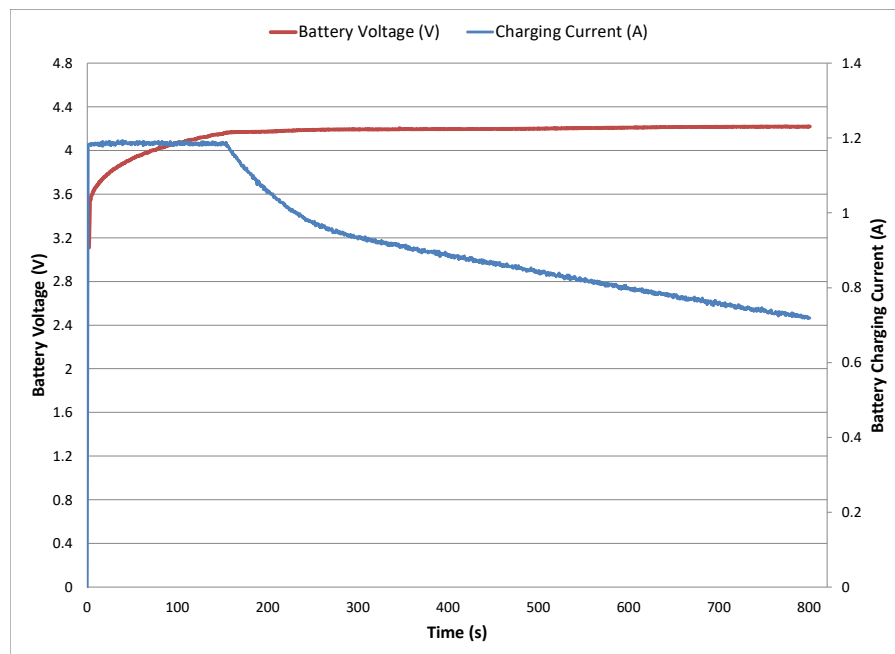


Figure 6.16: Constant current and constant voltage charging

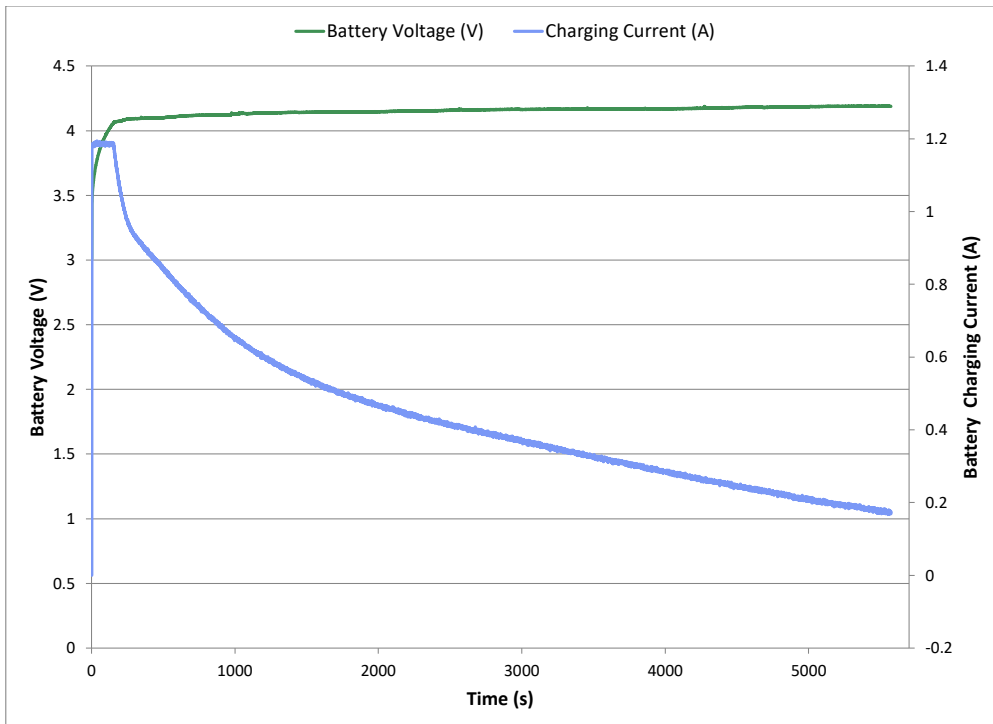


Figure 6.17: Variation of charging voltage and current while charging the 18650 Li-Ion battery upto 100%

6.5 MPPT Module Testing

The demo board for MPPT is designed with SPV1040T IC, which has a lower cutoff voltage of 1V. Varying input voltages from solar panel is estimated to be between 2 V-5 V. The MPPT board will boost voltages in these range to 5V or larger and provide it to the battery charger. The basic working of the MPPT board is tested by providing an input voltage between 2 V and 5 V and measuring the output voltage, which will be 5 V or more.

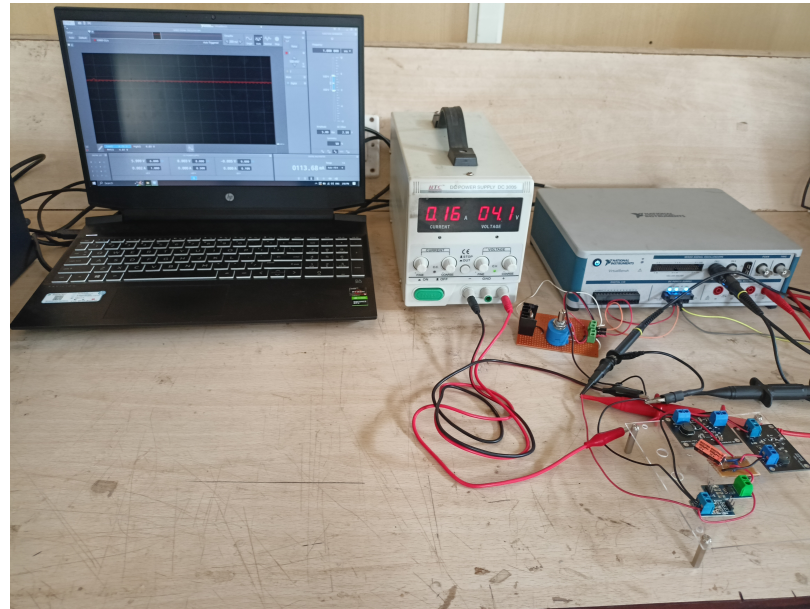


Figure 6.18: MPPT test setup

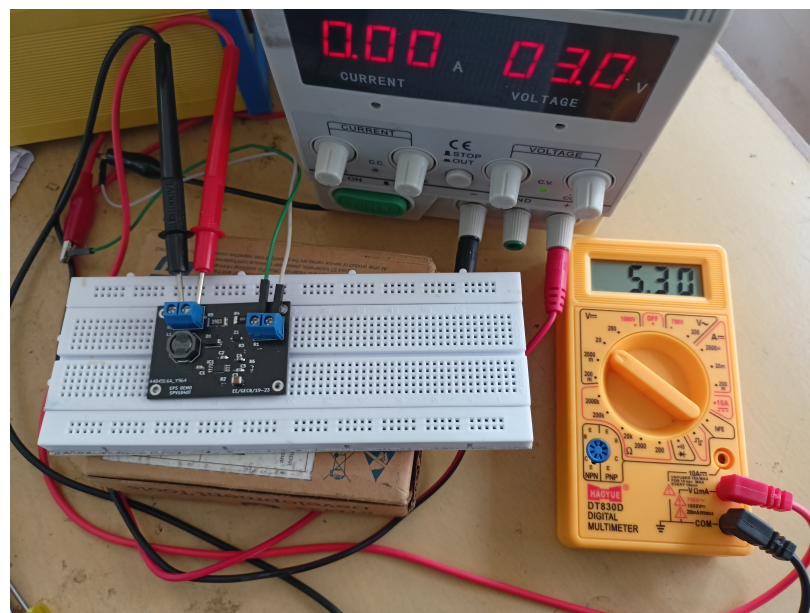


Figure 6.19: MPPT output voltage at no load

Vin (Volt)	Iin (A)	Vout (Volt)	Efficiency
2	0.4	3.55	88.75
2.5	0.35	3.9	89.14286
3	0.29	4.19	96.32184
3.3	0.28	4.38	94.80519
3.6	0.27	4.55	93.6214
4	0.26	4.8	92.30769
4.2	0.25	4.95	94.28571
4.6	0.24	5.11	92.57246

Table 6.12: MPPT output line regulation at half load (200 mA)

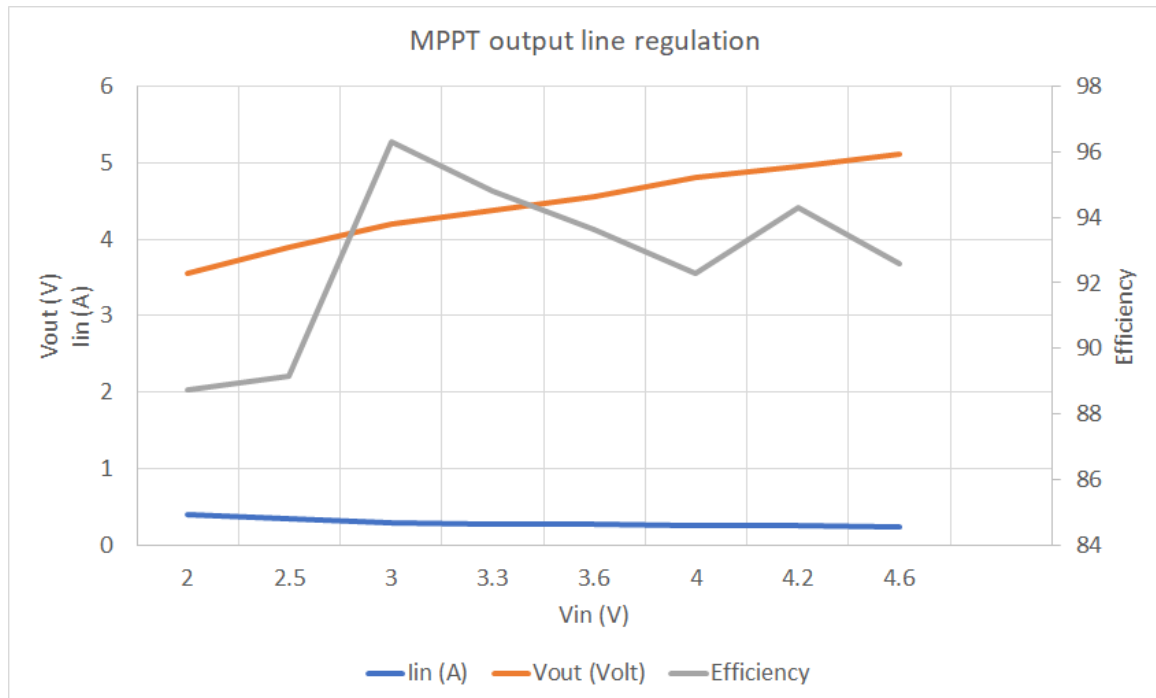


Figure 6.20: MPPT output line regulation at half load (200 mA)

Vin (Volt)	Iin (A)	Vout (Volt)	Efficiency
2	0.39	1.88	98.82051
2.5	0.43	2.48	94.58605
3	0.45	3.02	91.71852
3.3	0.46	3.39	91.56126
3.6	0.44	3.78	97.84091
4	0.45	4.2	95.66667
4.2	0.45	4.41	95.66667
4.6	0.49	5	90.94942

Table 6.13: MPPT output line regulation at full load (400 mA)

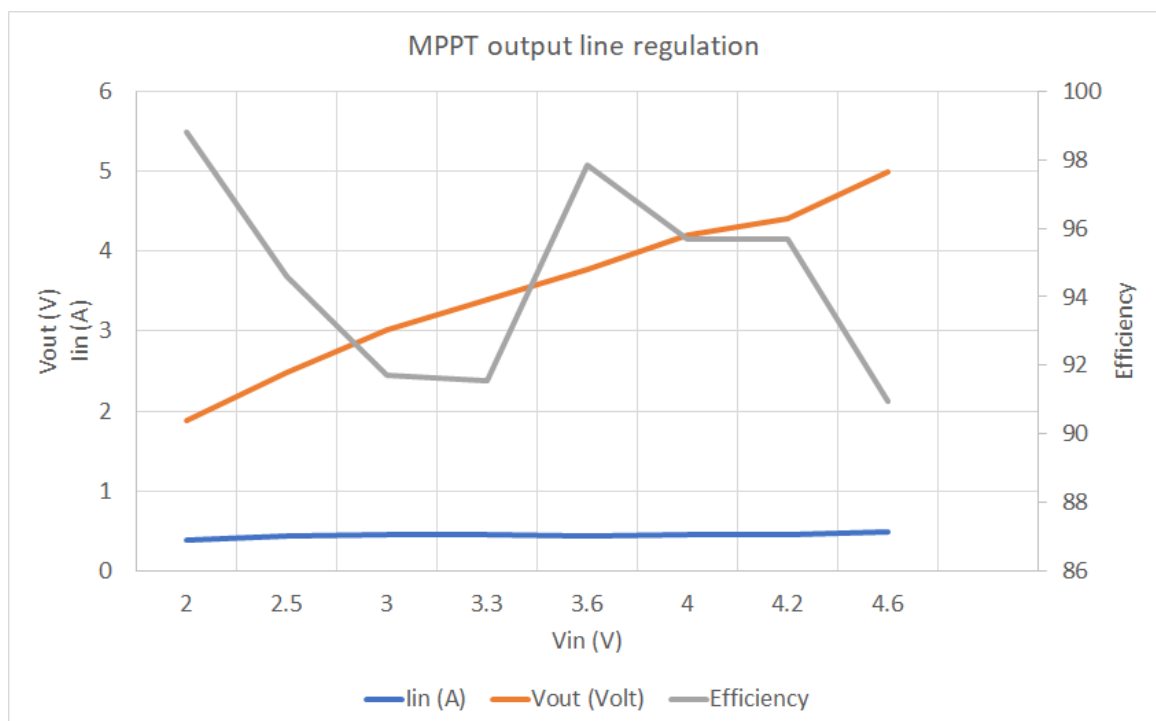


Figure 6.21: MPPT output line regulation at full load (400 mA)

Chapter 7

Conclusion

The work described here corresponds to the first phase of work on the development of the Electrical Power System of BARTOSAT. The objective was to carry the project forward as far as possible to build a base to design a fully functional EPS by selecting appropriate architecture and testing different sections of the EPS separately so that building a fully integrated EPS would become more easy.

7.1 Accomplished Work

7.1.1 Architecture

The architecture of the EPS as well as interaction between components are established. An EPS architecture with peak power transfer, regulated supply and distributed topology was selected and successfully implemented. An initial power budget was computed to calculate the total power consumption and to select appropriate voltage regulation IC's according to the maximum current output.

7.1.2 Design

Circuits for voltage regulation, i.e buck circuit, boost circuit, MPPT, battery charger with power path were designed and the PCB boards for the circuits were fabricated. The boards were also soldered successfully.

All the demo boards are integrated into a single PCB board, including the microcontroller, implementing PC/104 architecture. The schematic of the 4 layer PCB board schematic was also drawn and designed and footprints were assigned to the components.

7.1.3 Implementation and tests

The modules were tested properly to find the voltage regulation, load regulation characteristics and the results were plotted. Also, the efficiencies of all the modules were calculated at different operating conditions and plotted.

7.2 Future Scope

- Complete PCB routing of the 4 layer PCB.
- Update the power budget of the CubeSat by including new requirements of all the subsystems.
- Improve the design of the 5V and 3.3V converters to reduce voltage ripple by adding filter capacitors.
- Measure the I-V curve of the solar panels and compare the result with the MATLAB model.
- Design a battery heater for the final EPS board.
- Improve the design of protection circuit.
- Implement redundant circuit design.
- Test the EPS with all other subsystems, both in the laboratory and in appropriate environmental conditions.
- Test multitasking in STM32 micro-controller by implementing FreeRTOS.

REFERENCES

- [1] A. Edpuganti, V. Khadkikar, M. S. E. Moursi, H. Zeineldin, N. Al-Sayari and K. Al Hosani, "A Comprehensive Review on CubeSat Electrical Power System Architectures," in IEEE Transactions on Power Electronics, vol. 37, no. 3, pp. 3161-3177, March 2022, doi: 10.1109/TPEL.2021.3110002.
- [2] B. Hussein, A. M. Massoud and T. Khattab, "Centralized, Distributed, and Module-Integrated Electric Power System Schemes in CubeSats: Performance Assessment," in IEEE Access, vol. 10, pp. 55396-55407, 2022, doi: 10.1109/ACCESS.2022.3176902.
- [3] A. Edpuganti, V. Khadkikar, H. Zeineldin, M. S. E. Moursi and M. Al Hosani, "Comparison of Peak Power Tracking Based Electric Power System Architectures for CubeSats," in IEEE Transactions on Industry Applications, vol. 57, no. 3, pp. 2758-2768, May-June 2021, doi: 10.1109/TIA.2021.3055449.
- [4] Knap, Vaclav and Vestergaard, Lars and Stroe, Daniel-Ioan. (2020). A Review of Battery Technology in CubeSats and Small Satellite Solutions. Energies. 13. 4097. 10.3390/en13164097.
- [5] E. Ayoub and N. Karami, "Review on the charging techniques of a Li-Ion battery," 2015 Third International Conference on Technological Advances in Electrical, Electronics and Computer Engineering (TAECEC), 2015, pp. 50-55, doi: 10.1109/TAECEC.2015.7113599.
- [6] Robert W. Erickson, "Fundamentals of Power Electronics", Kluwer Academic Publishers, 1997
- [7] High efficiency solar battery charger with embedded MPPT, SPV1040, STMicroelectronics, 2021.
Available: <https://www.st.com/resource/en/datasheet/spv1040.pdf>
- [8] Standalone 1-Cell 2.0-A Buck Battery Charger, BQ25302, October 2020. Available: <https://www.ti.com/lit/ds/symlink/bq25302.pdf>
- [9] High-Efficiency, SOT23 Step-Down, DC-DC Converter, TPS62203, June 2015.
Available: <https://www.ti.com/lit/ds/symlink/tps62200.pdf>
- [10] 1.2MHz Step-Up DC/DC Converter in SOT-23, LTC3426, June 2017. Available: <https://www.analog.com/en/products/ltc3426.html>